CLIMATOLOGICAL SYNOPTIC PATTERNS OF TORNADO GENESIS IN EASTERN IDAHO

Thomas A. Andretta, William Wojcik, and Ken Simosko

National Weather Service Forecast Office

Pocatello-Idaho Falls, Idaho

Abstract

This study examines the climatological synoptic patterns that resulted in the genesis of tornadoes in eastern Idaho. Historical records of tornadic-related synoptic indicators originating from the Storm Prediction Center (SPC) and the Climate Diagnostics Center (CDC) spanned the 50 year period from 1954 to 2003. A total of 70 cases (with 88 individual reports) were analyzed with the following synoptic fields: 300 mb wind speed, 300 mb geopotential height, 300 mb temperature, 500 mb wind speed, 500 mb geopotential height, 500 mb temperature, 700 mb wind speed, 700 mb geopotential height, 700 mb temperature, 700 mb vertical velocity, surface to 500 mb wind shear, and mean sea-level pressure. High resolution spatial maps illustrating tornado location and intensity were developed to indicate the spatial distribution of the tornadoes. The temporal cycle of the tornadoes was divided into monthly and hourly dependent histograms. Tornadic events were collated into pattern types based on common synoptic signatures from the aforementioned climatic databases. Three synoptic patterns were identified: coastal trough-inland ridge, coastal ridge-inland trough, and zonal. Composite mean charts were developed from the various synoptic fields along with intuitive examples in order to illustrate the meteorological significance of each pattern type. By using such pattern recognition techniques, the operational forecaster will have a powerful tool to analyze weather patterns which precipitate the onset of a tornadic episode.

1. Introduction

Tornadoes in the Intermountain West are relatively rare occurrences with a climatological average of 2 to 3 tornadoes per year in the state of Idaho. The scientific literature is equally scarce with studies on tornadoes in the western United States. Fortunately, there have been some valuable research studies over the past two decades which have expanded the understanding of tornadoes in the Great Basin. For example, Fujita (1989) researched the damage paths related to the July 1987 F4 tornado in the Teton-Yellowstone Park (near the Idaho-Wyoming border). Evenson and Johns (1995) investigated the antecedent synoptic conditions associated with severe weather patterns in the Northwest United States. Evenson (1996) applied pattern recognition techniques (Evenson and Johns, 1995) to investigate severe weather events that occurred in July 1995. Bluestein (2000) documented a supercell tornado that formed over the mountains southwest of Denver, Colorado. Dunn and Vasiloff (2001) discussed the synoptic and mesoscale

conditions that resulted in a rare F2 tornado in Salt Lake City, Utah in August 1999. Most recently, Simosko and Hedges (2003) examined the synoptic conditions and radar signatures associated with a springtime F0 tornado near Pocatello, Idaho. There have been no other comprehensive studies regarding tornadoes in Idaho. This manuscript will concentrate on the synoptic environments associated with the development of tornadoes in eastern Idaho using several climatic databases.

2. Background

a. Topography

Figure 1a shows a map of the Northwest United States indicating the region of study with the red inset region highlighting the subdomain of interest. Figure 1b displays the topography map of eastern Idaho with county names and boundaries, including a topographic elevation legend. The main orographic feature in eastern Idaho is the Snake River Plain which is contoured in the shape of a bowl. The expansive plain is approximately 75 miles wide and is oriented from southwest to northeast with a gradual increase in elevation from ~1300 m MSL near Lincoln county to ~1500 m MSL in southern Fremont county. This distance covers nearly 150 miles. To the north and south of the Snake River Plain, there are higher basins and mountains that rise in elevation from 1700 to 3500 m MSL. Note the finger-like valleys oriented across Custer and Butte county that drain onto the upper part of the Snake River Plain in Bingham county. Similarly, there are north to south oriented valleys that allow winds to either drain out of or into the lower part of the Snake River Plain. The highest terrain is in Custer county where elevations rise to above 4000 m MSL. The topographic configuration in eastern Idaho is crucial to the development of numerous weather phenomena including: cyclonic vortices (Andretta and Hazen, 1998), post-cold frontal wind convergence zones (Andretta, 2002), and surface mesoscale boundaries (Simosko and Hedges, 2003).

3. Data Analysis

This tornado study employs local storm reports from the Storm Prediction Center (SPC) to garner tornado events over eastern Idaho defined by the geographical boundaries specified in Figure 1b. The historical time period of these events spanned the 50 year record from 1954 to 2003. Incidents of funnel clouds were excluded from the study. The SPC data were checked for consistency using similar data sets from the National Climatic Data Center (NCDC). A total of 70 cases covering 88 tornadic episodes were identified with the F0 to F2 tornado intensity (Fujita, 1981). No cases of tornadoes with an intensity higher than F2 (only 5 cases) were found in the data analysis. Dates that occurred within two hours of 0000 UTC were counted as two conjoined days (resulting in 94 cases) but one unique case (70 cases). High resolution spatial maps illustrating tornado location and intensity were developed to indicate the spatial distribution of the tornadoes. The temporal cycle of the tornado frequency was organized into monthly and hourly dependent histograms.

Once these 70 cases were collected, National Center for Environmental Prediction (NCEP)

Reanalysis data provided by the NOAA-CIRES Climate Diagnostics Center (CDC) [http://www.cdc.noaa.gov/], were used to correlate synoptic patterns to each of the tornadic episodes (Kalnay et. al., 1996). The decision to collate a synoptic pattern to a tornadic event was based on an initial examination of the 500 mb geopotential height pattern. Once a pattern match was found, other synoptic fields were collected for further comparison and study including: 300 mb wind speed, 300 mb geopotential height, 300 mb temperature, 500 mb wind speed, 500 mb temperature, 700 mb wind speed, 700 mb geopotential height, 700 mb temperature, 700 mb vertical velocity, surface to 500 mb wind shear, and mean sea-level pressure. Unfortunately, other germane fields like vorticity and helicity were not available in the CDC data repository. Each synoptic field in the CDC database represented a composite (average) of the long-term mean for each day.

The superimposed epoch method (Panofsky and Brier, 1965; Wilks, 1995) which involves vertical analysis of various synoptic fields (e.g., height, temperature, and wind) at a particular time step was used to analyze the fields of each synoptic pattern for correlation. First, a set of mean charts was obtained for each synoptic field in each analogue pattern. For example, the coastal ridge-inland trough 300 mb wind speed pattern was deduced by summing all 32 cases for that variable and dividing by 32. Likewise, the zonal 500 mb temperature pattern was deduced by summing all 6 cases for that variable and dividing by 6. Next, the 300 mb mean height, wind, and temperature maps were constructed at these times: day - 3 (D - 3), day - 2 (D - 2), day - 1 (D - 1), and day - 0 (D - 0). The same paradigm was applied to the 500 mb temperature and mean sea-level pressure fields for each of the documented synoptic regimes. The result was a 4 day evolution of various synoptic fields critical to the identification of a composite pattern associated with tornado genesis in eastern Idaho.

4. Results

a. Histograms

As indicated in Figure 2, there was a total of 88 individual tornadoes collected for the 70 cases; the majority of tornadoes occurred in Bingham, Jefferson, and Power counties. No tornadoes with an intensity above F2 were recorded in the data. Figure 3 shows that 60% of all eastern Idaho tornadoes were of the weak (F0) scale with 34% (F1) and 6% (F2) intensities, respectively (Fujita, 1981). The seasonal cycle of tornado genesis favored the summer months with 57% of all cases occurring between June and August (Figure 4). The hourly temporal distribution (Figure 5) revealed that most tornadoes occurred in the afternoon hours, between 1300 (100 PM) and 1800 (600 PM) LST. The peak occurrence (23%) was at 1600 (400 PM) LST; tornadic observations in the morning and twilight hours were very rare.

b. Maps

The spatial distribution of the Fujita tornado intensities for the 50 year climatological period from 1954 to 2003 is illustrated in Figure 6a. The figure indicates that of the 88 reports of tornadoes (including 11 multiple reports for a single event), the majority of the events were situated geographically in and along the valley walls of the Snake River Plain, collocated with the most densely populated centers in the region. There were no reports of tornadoes in Custer

county (Figure 1) but this may be indicative of the scarcity in population. Only 5 F2 reports (red triangles) were observed in the 50 year historical record and 2 of these reports occurred in Minidoka county. As indicated in Figure 6b, there was no correlation of the individual tornadic climatological synoptic patterns with location.

c. Composite Mean Charts

In all instances, the composite maps in the following figures were provided by NOAA-CIRES Climate Diagnostics Center, Boulder Colorado from their web site [http://www.cdc.noaa.gov/]. The CDC analysis (Figure 7) revealed three synoptic patterns associated with tornado genesis in eastern Idaho: coastal trough-inland ridge (CTIR: 32 cases), coastal ridge-inland trough (CRIT: 32 cases), and zonal (ZNL: 6 cases) patterns. Of the 5 F2 tornadic events, the CTIR and CRIT patterns were responsible for 3 and 2 episodes, respectively.

i. Coastal Trough-Inland Ridge (CTIR) Pattern

Figure 8 shows the three panel layout for the CTIR 300 mb pattern. The (geopotential) heights east of 150W are generally zonal as they move onshore with a broad 300 mb ridge tilted negatively back across Colorado into Idaho. The 300 mb temperatures are between -41 and -44 ^{o}C over eastern Idaho. The 300 mb jet stream pattern was concave-shaped, arching from the Pacific Ocean (40 to 50N) into coastal central California and nosing into eastern Idaho. The 500 mb pattern (Figure 9) for heights, temperatures, and wind speeds corresponds closely to the 300 mb pattern. The surface to 500 mb wind shear maximum (Figure 9d) follows the symmetry of the 300 and 500 mb wind speed patterns and is aligned across Oregon into central Idaho. The 700 mb charts (Figure 10) reveal a pronounced height and thermal ridge over eastern Idaho. There is a deep negatively-tilted 700 mb coastal trough with a broad ridge over eastern Idaho. Like the 300 and 500 mb wind speed panels, the 700 mb jet stream (Figure 10c) noses into Idaho from the coastal regions of central California. Note the 700 mb vertical velocity maxima over southern Idaho and Nevada in Figure 10d.

The temporal progression of the 300 mb mean height pattern in Figure 11 indicates a backing of the winds with time from a westerly trajectory at day - 3 to a southwesterly flow by day - 0. The 300 mb wind speed mean charts (Figure 12) indicate a wind speed maximum (34 to 40 m s^{-1}) across Montana by day - 3 but by day - 0, this feature moves east of Idaho. All of eastern Idaho remains under a broad regime of 28 to 35 m s^{-1} wind speeds for all 4 days with the right rear entrance region of the 300 mb jet stream over the region. The 500 mb temperature pattern (Figure 13) reveals a tight thermal packing off the western United States with a 500 mb temperature ridge located over Idaho. As the tornadic event approaches the time of day - 1, the upper-level flow changes with the ridge axis replaced by a negatively-tilted cold trough axis just upstream of Idaho. The mean sea-level pressure pattern in Figure 14 indicates a slow deepening trend over the 4 day period in the Great Basin with a contour of 1010 mb over westem Idaho by day - 0. The composite mean chart for the CTIR pattern is illustrated in Figure 15. In fact, this pattern resembles the Pattern B SSWE discussed by Evenson and Johns (1995). An example of some of the synoptic fields associated with the CTIR pattern is given in Figure 16 for the 2000 February 14-15 tornadic event. Of noteworthy significance, this event was associated with several F0 and F1 tornadoes that touched down in Power and Bannock counties (Figure 1b) and originated from a large bow echo (Burke and Schultz, 2003). A broad trough axis at both 300

and 700 mb is situated near 137W. There are 300 and 700 mb jet maxima rotating across southern Idaho in the broad anticyclonic flow over Idaho and Utah.

ii. Coastal Ridge-Inland Trough (CRIT) Pattern

Figure 17 indicates a three panel layout of the 300 mb CRIT pattern. An inspection of the data shows that the 300 mb trough is situated just west of Idaho in Figure 17a. Note the -42 to -45 ^{o}C line in Figure 17b indicating the cold air aloft over the region. The most striking pattern is the 300 mb wind field – with a double jet structure described as one wind speed maximum off the Oregon coast (back side of trough) and an even stronger one over Utah (front side of trough). A region of 44 to 50 m s^{-1} (Figure 17c) is indicated over Utah with eastern Idaho in the favorable lifting region associated with upper-level divergence in the left front exit region of the jet stream. The 500 mb pattern provides similar clues in Figure 18. The 500 mb (geopotential) height and temperature axes are located along the Idaho-Oregon border in both Figures 18a and 18b. Like the 300 mb pattern, a wind maximum is present in Utah with eastern Idaho in the left front exit region of the 500 mb jet stream (Figure 18c). The surface to 500 mb wind shear pattern (Figure 18d) shows the axis of shear nosing into Idaho from Montana and Wyoming. The 700 mb height, thermal, and wind speed patterns are reflective of the upper-level signatures. Figures 19a and 19b show the 700 mb height and trough axes situated near the Idaho-Oregon border in the CRIT pattern. Like the 300 and 500 mb patterns, the depth of the trough at 700 mb extends into Nevada and coastal southern California. The wind speed pattern at 700 mb displayed in Figure 19c shows a maximum (20 to 25 m s^{-1}) off the Oregon coast. Figure 19d illustrates the 700 mb omega maximum centered over Idaho and Utah for the CRIT pattern.

The 300 mb height pattern for days 3, 2, 1, and 0 days prior to the onset of the CRIT pattern is analyzed in Figure 20. Note that the trough height pattern deepens as it progresses inland. This would be expected as the winds on the back side of the trough axis strengthen and deepen the trough amplitude with time (Figure 21). The 300 mb wind speed pattern shows a rapid intensification of the wind speeds off the coast by day - 1 and day - 0 between 45 and 55N. The 500 mb temperature pattern (Figure 22) for the 4 day evolution shows the thermal gradient increasing with time over Idaho and Utah as the upper trough moves onshore by day - 1. The mean sea-level pattern in Figure 23 reveals a broad pressure minimum over the Intermountain West. There is no clear temporal connection among the various days. The composite mean chart for the CRIT pattern is illustrated in Figure 24. An example of some of the synoptic fields is displayed in Figure 25 for the 1991 May 18 tornadic event which was associated with an F2 tornado over Minidoka county. There were closed 300 and 700 mb low pressure systems located over the Great Basin with height minima over northern Nevada. The double jet structure is a salient characteristic of this synoptic signature in Figures 25b and 25d. Note the 300 mb jet maximum that noses into Utah with southern Idaho on the left front quadrant of the 300 mb jet maximum. There is a south low-level jet maximum over eastern Idaho and Utah with a veering of the winds aloft to a southwest direction over Utah.

iii. Zonal (ZNL) Pattern

The Zonal pattern in Figure 26 illustrates the prevailing horizontal alignment of the (geopotential) height and temperature contours. The 300 mb temperatures are -41 to -44 ^{o}C over eastern Idaho in this pattern. The most interesting aspect is the 50 to 60 m s^{-1} jet maximum

which extends from 40 to 50N in the Pacific Ocean and noses onshore into Oregon and Idaho. This jet maximum is stronger in magnitude versus similar maxima in the CTIR and CRIT synoptic patterns. The 500 mb pattern (Figure 27) shows the onshore flow with the surface to 500 mb wind shear maximum nosing into western Idaho. A similar trend is manifested in the 700 mb height, temperature, and wind speed data in Figure 28. Note the large region of positive lift (Figure 28d) over Washington, Oregon, and Idaho.

The 300 mb mean height temporal sequence in Figure 29 shows the development of an upper-level trough off the coast of British Columbia by day -1 and day - 0. This has the net effect of lowering the heights slightly over eastern Idaho. The 300 mb mean wind speed charts in Figure 30 show an illuminating daily progression. In day - 3 and day - 2, a speed maximum becomes oriented meridionally from Vancouver Island to northern Idaho. As the tornadic event approaches day - 0, this feature is replaced by a powerful onshore jet maximum (46 to 54 m s^{-1}) which noses into Idaho. The 500 mb mean temperature charts in Figure 31 reveal the formation of a low pressure trough over British Columbia by day - 1 and day - 0. The mean sea-level pressure charts (Figure 32) indicate pressure minima forming over Manitoba and Utah by day - 0. The composite mean chart for the Zonal pattern is illustrated in Figure 33. An example of some of the synoptic elements is given in Figure 34 for the 1988 March 23 tornadic event. This event was associated with an F1 tornado in Jefferson county. Note the tight height gradient offshore between 40 and 45N (west of 130W) in both the 300 and 700 mb patterns. This pattern transforms into a negatively-tilted upper trough over Vancouver Island with a 300 mb jet maximum nosing into northern Idaho.

5. Conclusions

This study explored the tornado climatology of eastern Idaho. A total of 88 individual tornadoes was collected for 70 cases; the majority of tornadoes occurred in Bingham, Jefferson, and Power counties. No tornadoes with an intensity above F2 were recorded in the data. Most (60%) tornadoes in eastern Idaho were of the weak (F0) variety. The tornado seasonal cycle favored the summer months with 57% of all cases occurring between June and August. The hourly temporal distribution revealed that most tornadoes occurred in the afternoon hours, between 1300 (100 PM) and 1800 (600 PM) LST. The peak occurrence (23%) was at 1600 (400 PM) LST; tornadic observations in the morning and twilight hours were extremely rare.

Furthermore, the spatial distribution of tornadoes for the 50 year climatological period from 1954 to 2003 indicated that of the 88 reports of tornadoes (including 11 multiple reports for a single event), the majority of the events were situated geographically in and along the valley walls of the Snake River Plain, collocated with the most densely population centers. There were no reports of tornadoes in Custer county, reflective of the low population density. Only 5 F2 reports were observed in the 50 year historical record and 2 of these reports occurred in Minidoka county. (The CTIR and CRIT patterns were responsible for 3 and 2 F2 incidents, respectively.) There was no correlation of the individual tornadic climatological synoptic patterns with location.

Finally, this paper investigated antecedent synoptic conditions that resulted in tornadoes in eastern Idaho. Results obtained from the Climate Diagnostics Center (CDC) repository revealed

3 synoptic patterns associated with tornado genesis in eastern Idaho: coastal trough-inland ridge (32 cases), coastal ridge-inland trough (32 cases), and zonal (6 cases) patterns. Composite mean charts were constructed to assist the operational meteorologist in identifying each pattern and predicting the onset of a tornadic event. All patterns were characterized by a 300 mb temperature range of -41 to -45 ^{o}C over eastern Idaho. The CTIR pattern featured a southwest flow aloft over Idaho and a single jet maximum while the CRIT pattern was delineated by a double jet structure at 300 mb just upstream of Idaho. The Zonal pattern featured a westerly onshore flow with the 300 jet maximum nosing into eastern Idaho. An example of each of these synoptic patterns was described using height and wind elements from the 300 and 700 mb levels. By using such pattern recognition techniques, the operational forecaster will have a powerful tool to evaluate weather patterns which precipitate the onset of a tornadic episode.

6. References

Andretta, T. A., and D. S. Hazen, 1998: Doppler Radar Analysis of a Snake River Plain Convergence Event. *Wea. Forecasting*, **13:2**, 482-491.

Andretta, T. A., 2002: Climatology of the Snake River Plain Convergence Zone, *Natl. Wea. Dig.*, **26:3**, **4**, 37-51.

Bluestein, H. B., 2000: A Tornadic Supercell over Elevated, Complex Terrain: The Divide, Colorado, Storm of 12 July 1996. *Mon. Wea. Rev.*, **128:3**, 795–809.

Burke, P. C., and D. M. Schultz, 2003: A Climatology of Cold-Season Bow-Echoes over the Continental United States. *Wea. Forecasting*, submitted.

Dunn, L. B., and S. V. Vasiloff, 2001: Tornadogenesis and Operational Considerations of the 11 August 1999 Salt Lake City Tornado as Seen from Two Different Doppler Radars. *Wea. Forecasting*, **16:4**, 377–398.

Evenson, E. C., and R. H. Johns, 1995: Some Climatological and Synoptic Aspects of Severe Weather Development in the Northwestern United States: *Natl. Wea. Dig.*, **20:1**, 34-50.

Evenson, E. C., 1996: The 6 July and 9 July 1995 Severe Weather Events in the Northwestern United States: Recent Examples of SSWEs: NOAA Technical Memorandum NWS WR-237.

Fujita, T. T., 1981: Tornadoes and Downbursts in the Context of Generalized Planetary Scales. *J. Atmos. Sci.*, **38:8**, 1511–1534.

Fujita, T. T., 1989: The Teton-Yellowstone Tornado of 21 July 1987. *Mon. Wea. Rev.*, **117:9**, 1913-1940.

Kalnay, E. and Coauthors, 1996: The NCEP/NCAR 40-Year Reanalysis Project. *Bull. Amer. Meteor. Soc.*, **77:3**, 437-471.

Panofsky, H. A., and W. G. Brier, 1965: Some Applications of Statistics to Meteorology. The Pennsylvania State University, University Park, PA, 224 pp.

Simosko, K. and J. Hedges, 2003: Analysis of an F0 Tornado Using the Weather Event Simulator (WES). Western Region Technical Lite Attachment No. 03-39.

Wilks, D. S., 1995: Statistical Methods in Atmospheric Sciences. Academic Press, San Diego, ISDN 0-12-751965-3, 464 pp.

Acknowledgements

The authors wish to thank the Storm Prediction Center (SPC) and National Climate Data Center (NCDC) for providing the local storm reports of tornado incidents for eastern Idaho. The composite maps used in this study were provided by NOAA-CIRES Climate Diagnostics Center, Boulder Colorado from their web site [http://www.cdc.noaa.gov/]. The authors would like to thank several reviewers, especially Dr. Mike Brown of Mississippi State University, for constructive comments on this manuscript. The high resolution terrain maps featured in the planar analysis were provided by ISU student Dan Narsavage.

Authors

Thomas Andretta received his Bachelor of Science (1988) and Master of Science (1991) degrees in Atmospheric Science at the State University of New York (SUNY) at Stony Brook. His National Weather Service career has included a meteorologist intern at Lake Charles, LA (1993), journeyman meteorologist at Pocatello, ID (1995), and senior meteorologist at Pocatello, ID (1998). Mr. Andretta has lead authored two journal papers on the Snake River Plain Convergence Zone (SPCZ); he has also coauthored other studies on precipitation and snowfall climatology of eastern Idaho. His interests include boundary layer meteorology in complex terrain, fog physics, mesoscale precipitation processes, snowfall climatology, and tornado climatology. He enjoys designing meteorological applications on multiple computer platforms.

William Wojcik received his Bachelor of Science degree in Meteorology at the State University of New York (SUNY) at Oswego in 1991. He then attended the South Dakota School of Mines and Technology where he received a Master of Science degree in Atmospheric Sciences in 1994. In October 1994, Mr. Wojcik joined the National Weather Service as a meteorologist intern in Phoenix, AZ. He accepted a journeyman forecaster position in January 1999 at the National Weather Service office in Pocatello, ID. He has coauthored one journal paper and several research studies.

Ken Simosko received his Bachelor of Science (1989) in Meteorology at Millersville University in Lancaster, Pennsylvania. After working for a private weather company, he joined the Air Force where he was commissioned a 2nd Lt. Weather Officer in April 1991. By the late 1990s, he migrated to the private sector again working as a broadcast meteorologist at TV station KIDK in Idaho Falls, ID. Among his accomplishments, Mr. Simosko earned the Broadcasting Seal of

Approval from the American Meteorological Society. He joined the National Weather Service as a meteorologist intern (2002) and was quickly promoted to journeyman meteorologist (2003) at the forecast office in Pocatello, ID. His future ambitions include working towards becoming a National Weather Service senior meteorologist.

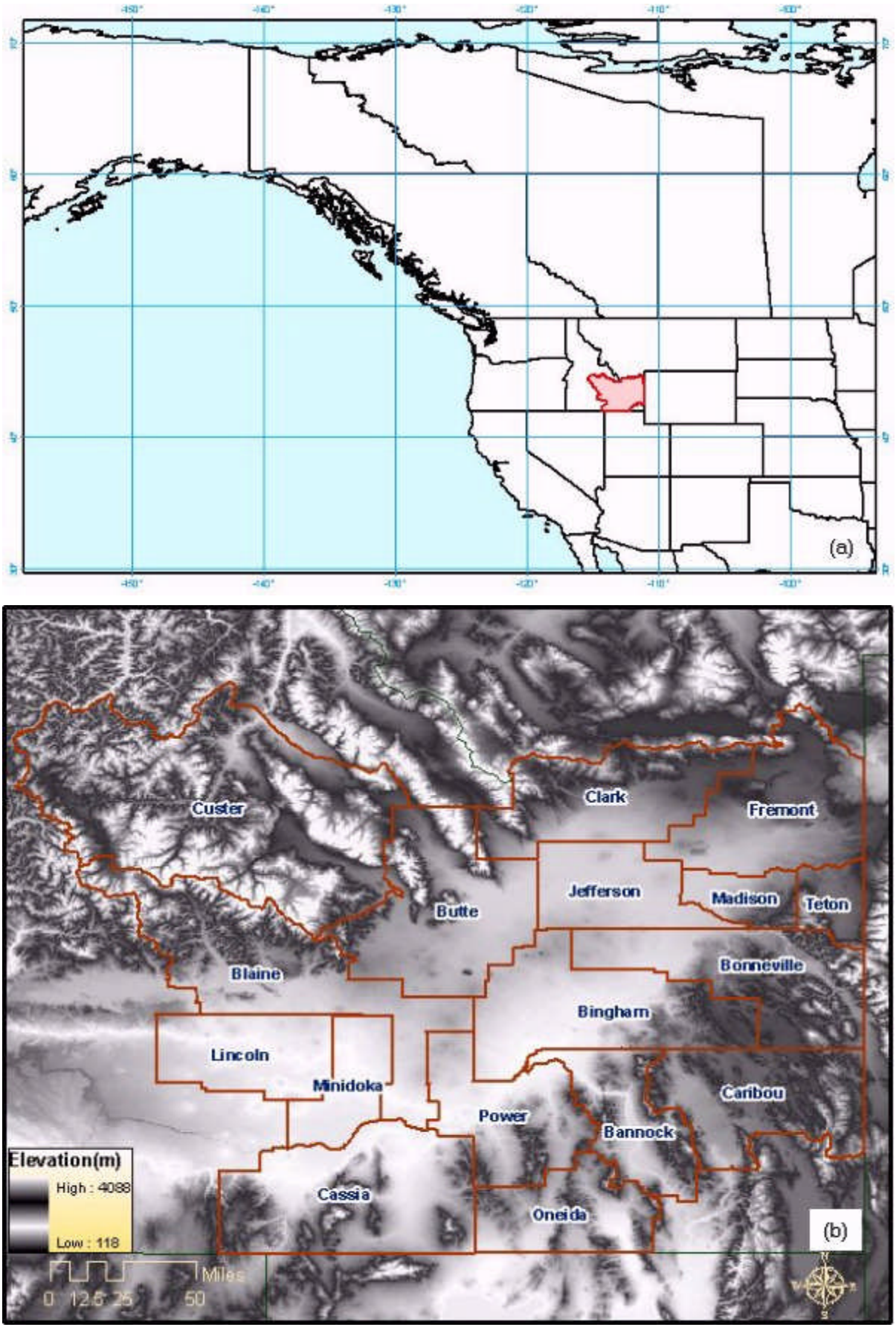

Figure 1: (a) Map of Northwest United States with inset (red) region of study
(b) Eastern Idaho domain with county outlines and names

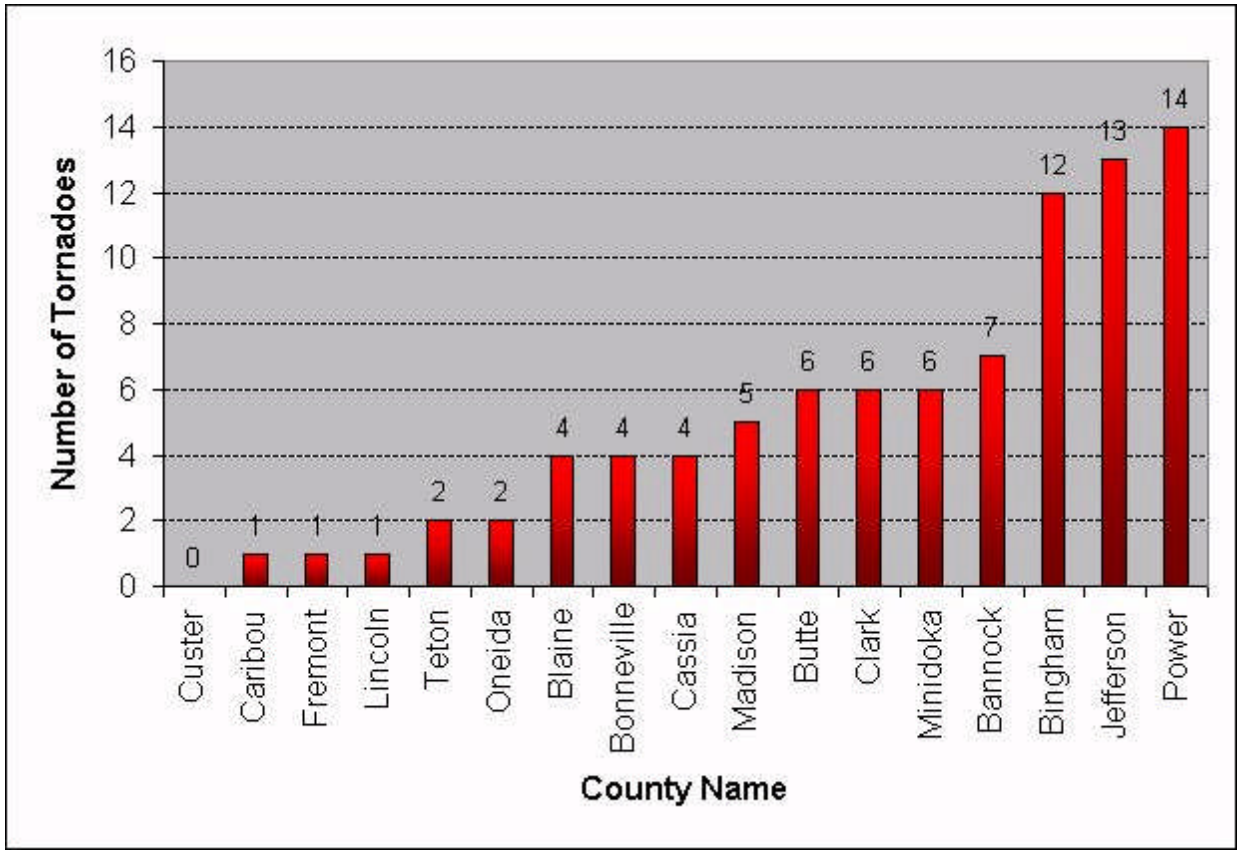

Figure 2: Histogram of eastern Idaho tornadoes by Idaho county

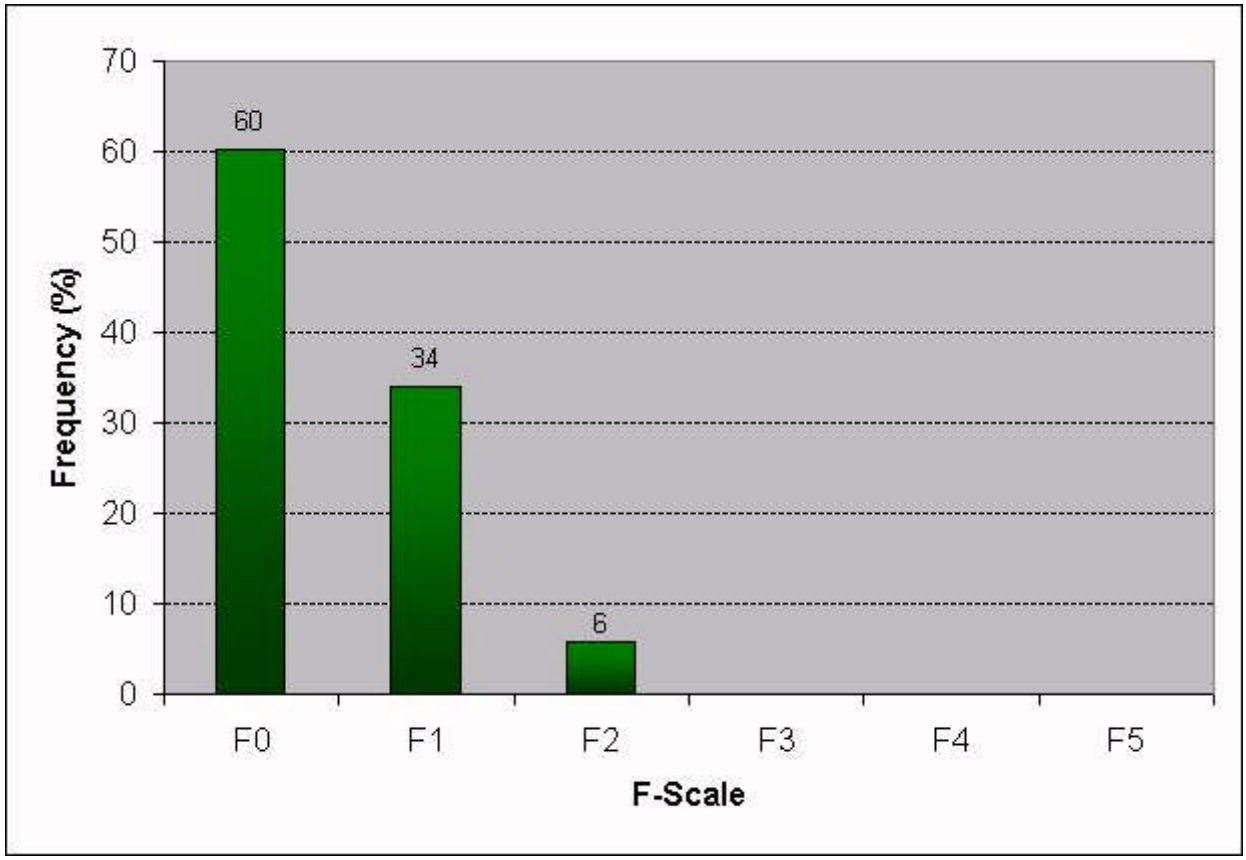

Figure 3: Histogram of eastern Idaho tornadoes by intensity

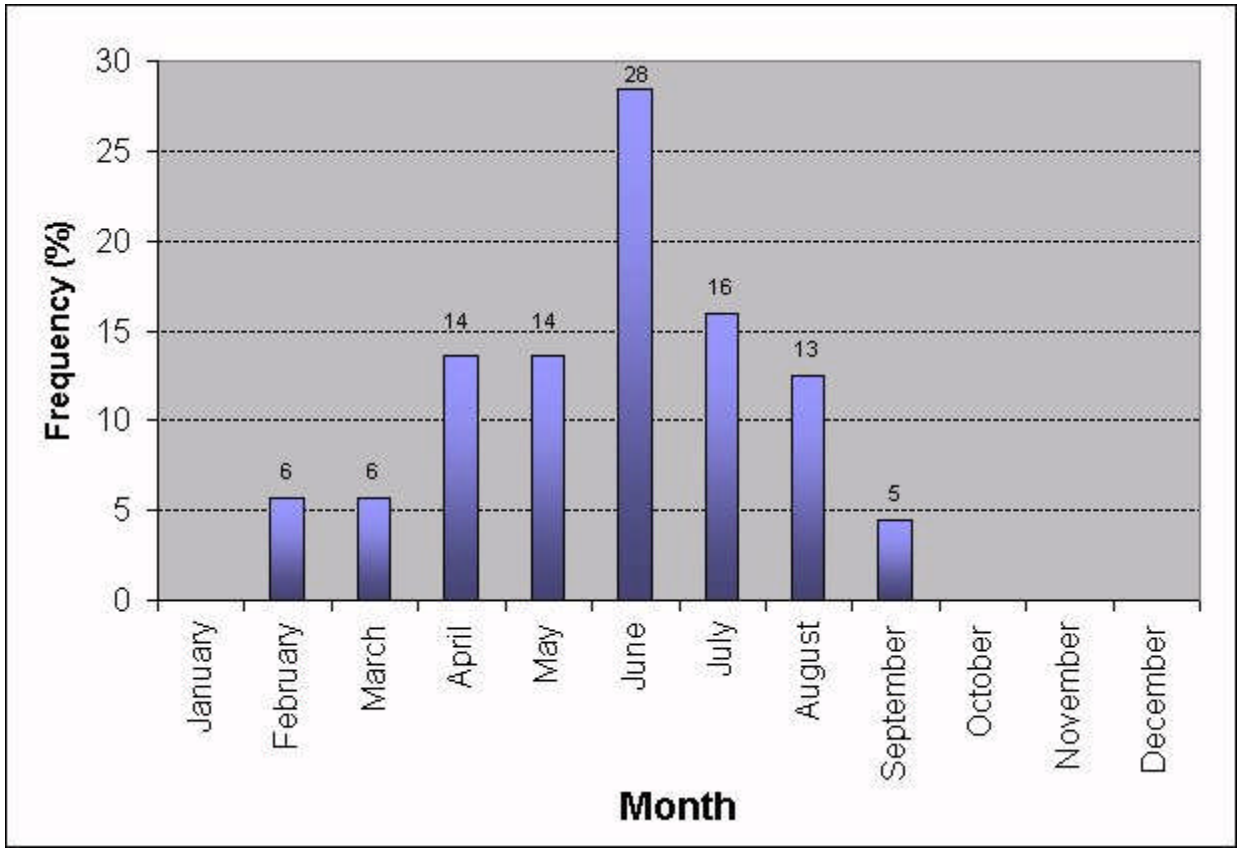

Figure 4: Histogram of eastern Idaho tornadoes by month

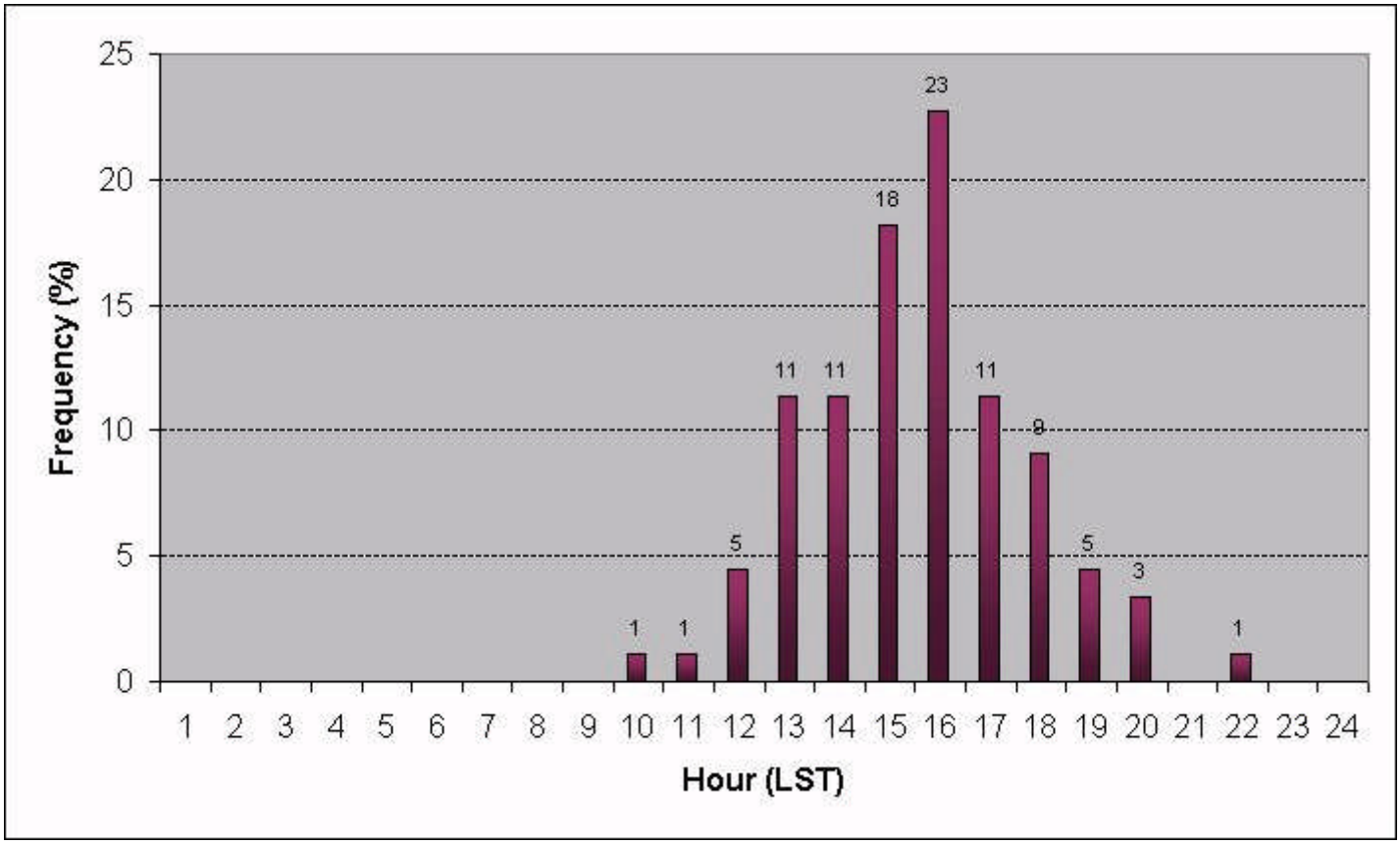

Figure 5: Histogram of eastern Idaho tornadoes by hour

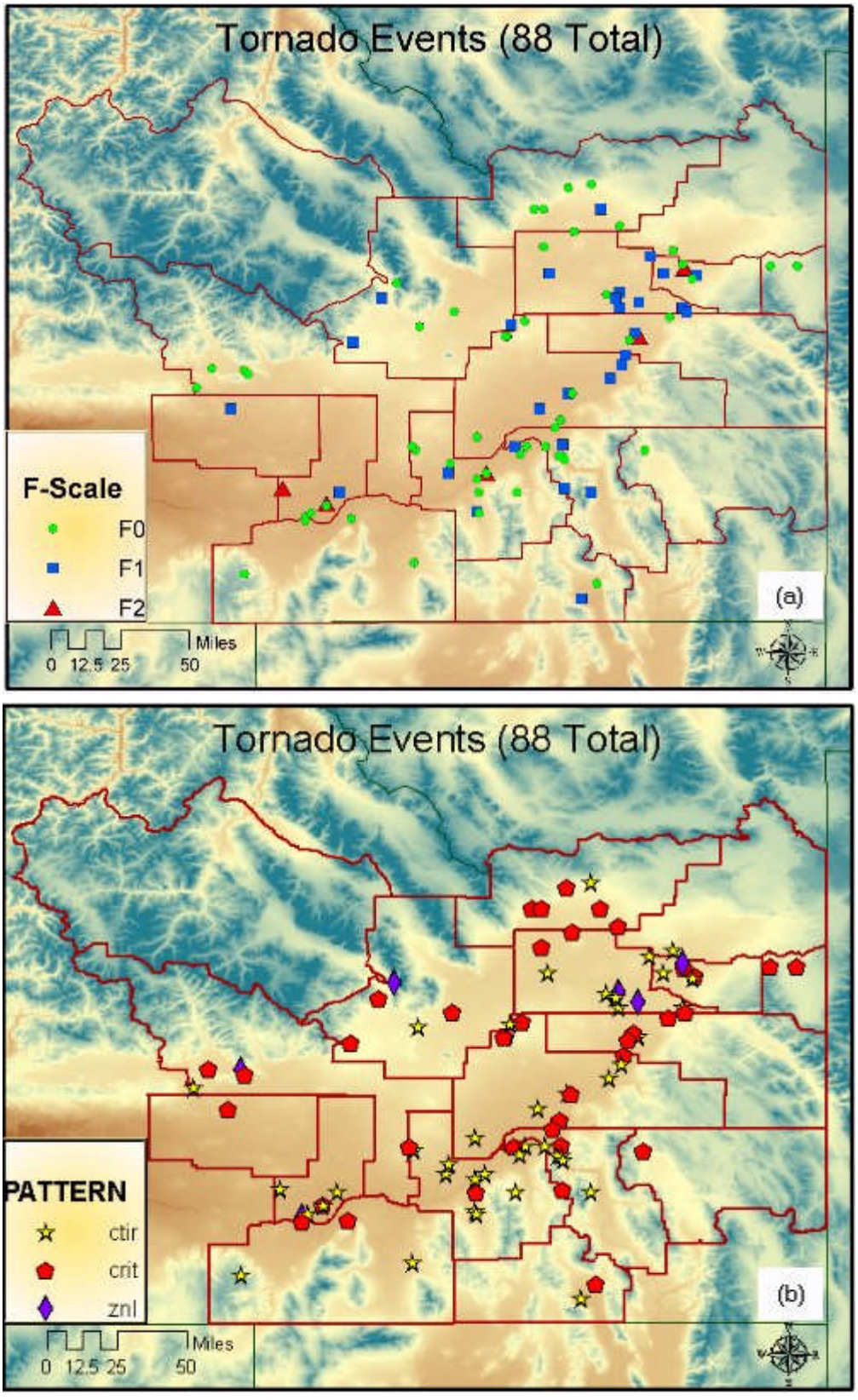

Figure 6: (a) Map of eastern Idaho with Fujita tornado intensity scales
(b) Map of eastern Idaho with climatological synoptic patterns

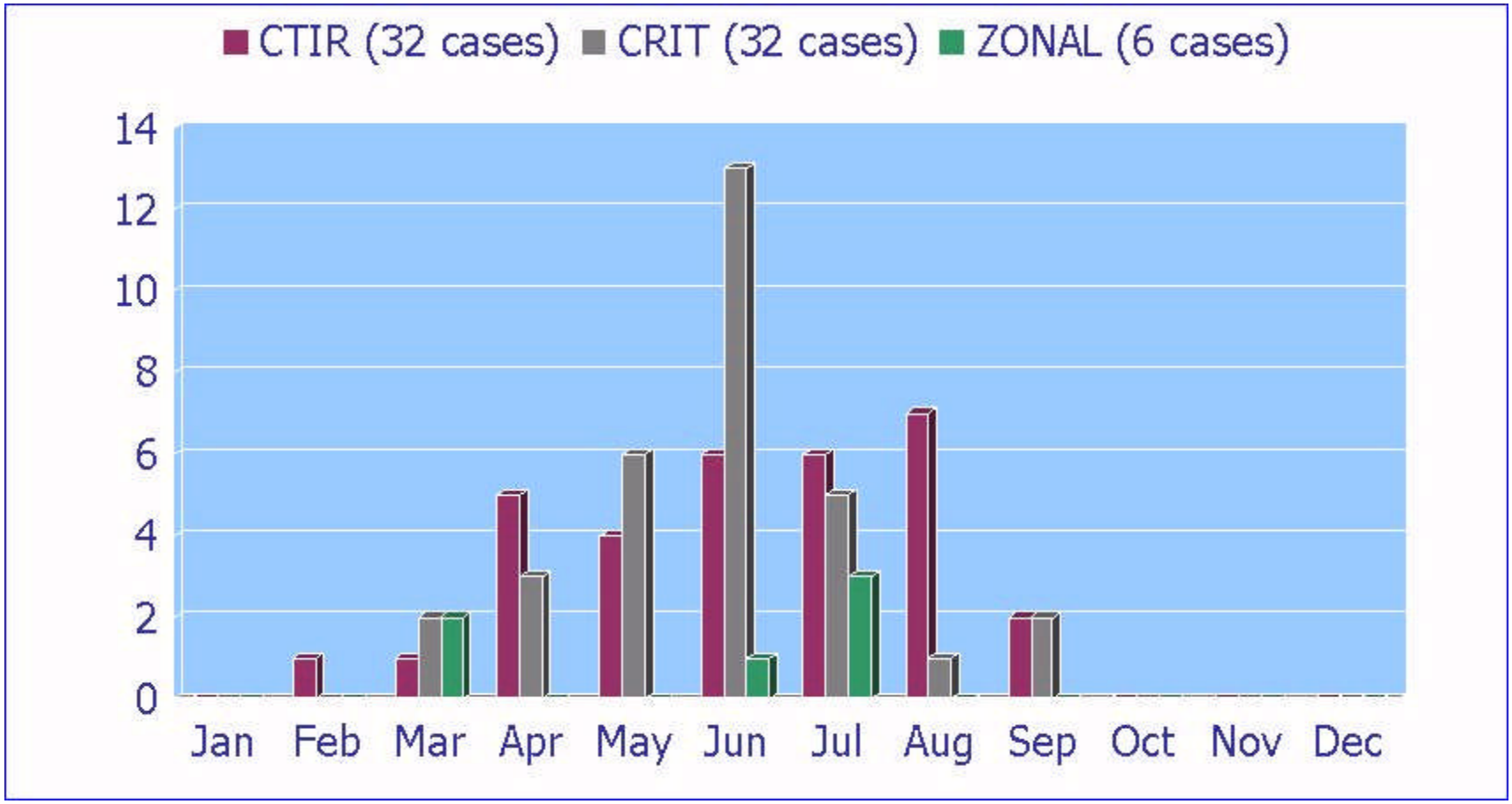

Figure 7: Histogram of tornado synoptic patterns

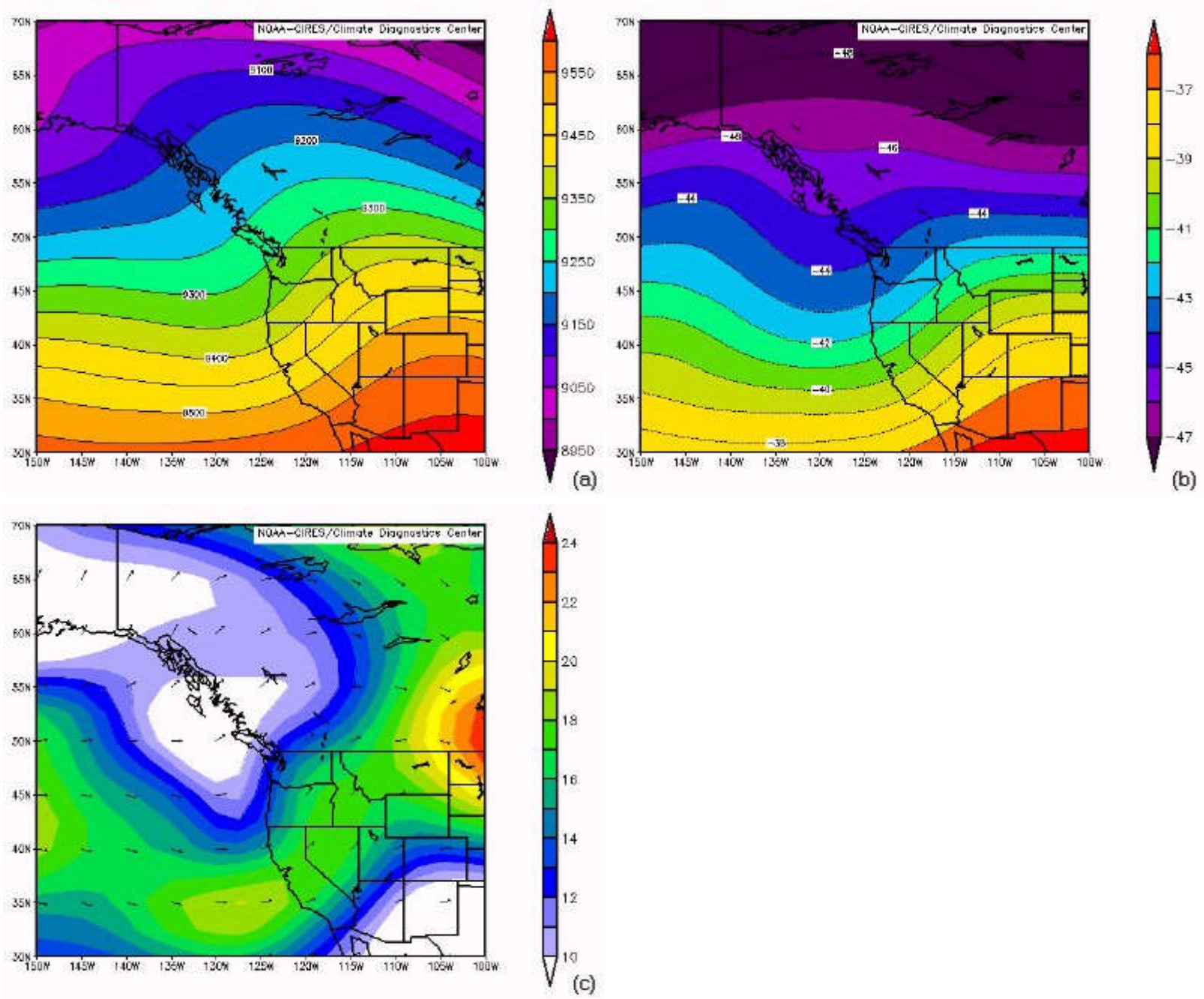

Figure 8: (a) Coastal Trough-Inland Ridge 300 mb height mean (m)
(b) Coastal Trough-Inland Ridge 300 mb temperature mean (^{o}C)
(c) Coastal Trough-Inland Ridge 300 mb wind speed mean (0.5 * m s^{-1})

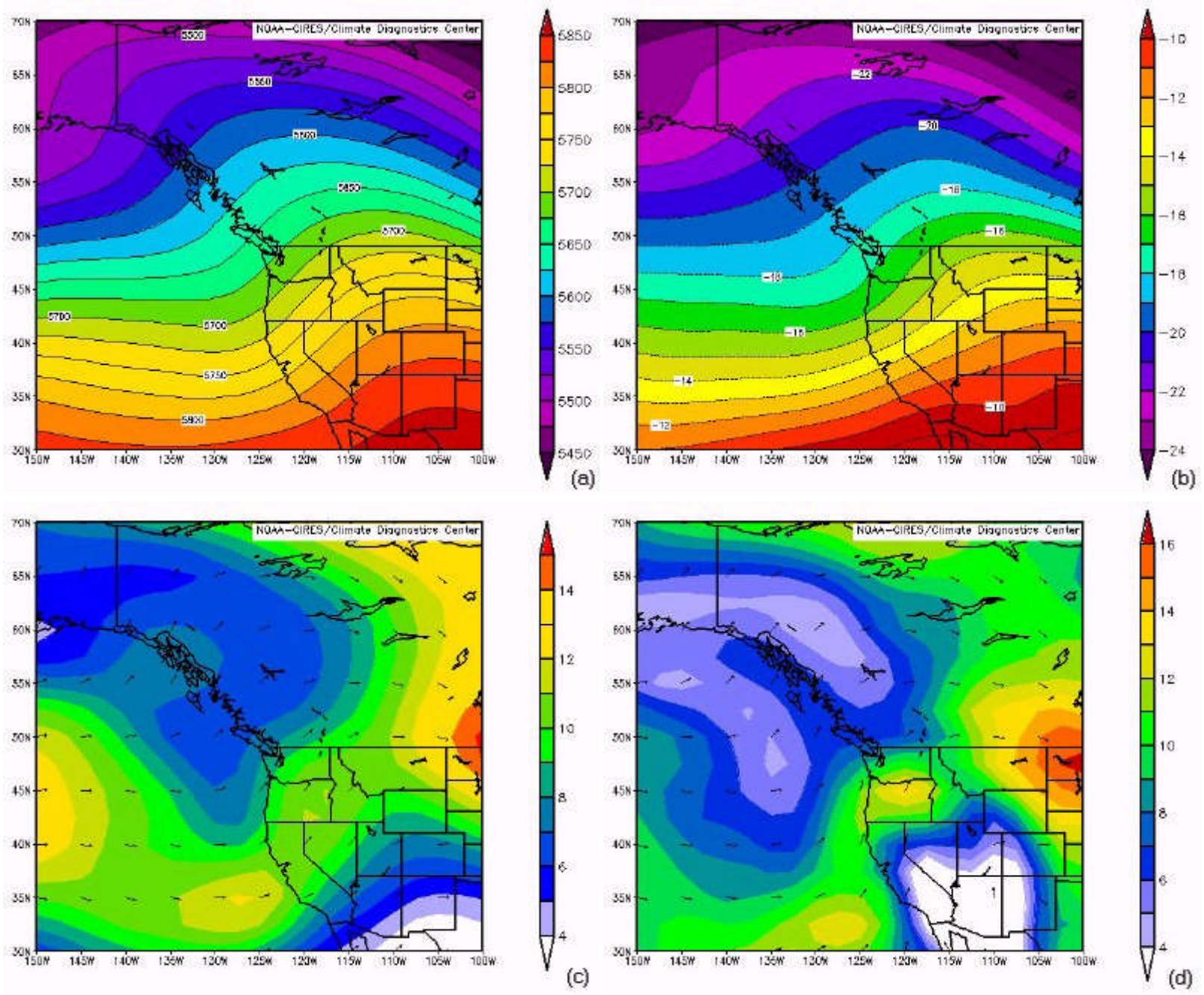

Figure 9: (a) Coastal Trough-Inland Ridge 500 mb height mean (m)
(b) Coastal Trough-Inland Ridge 500 mb temperature mean (^{o}C)
(c) Coastal Trough-Inland Ridge 500 mb wind speed mean (0.5 * m s^{-1})
(d) Coastal Trough-Inland Ridge surface to 500 mb wind shear mean (0.5 * m s^{-1})

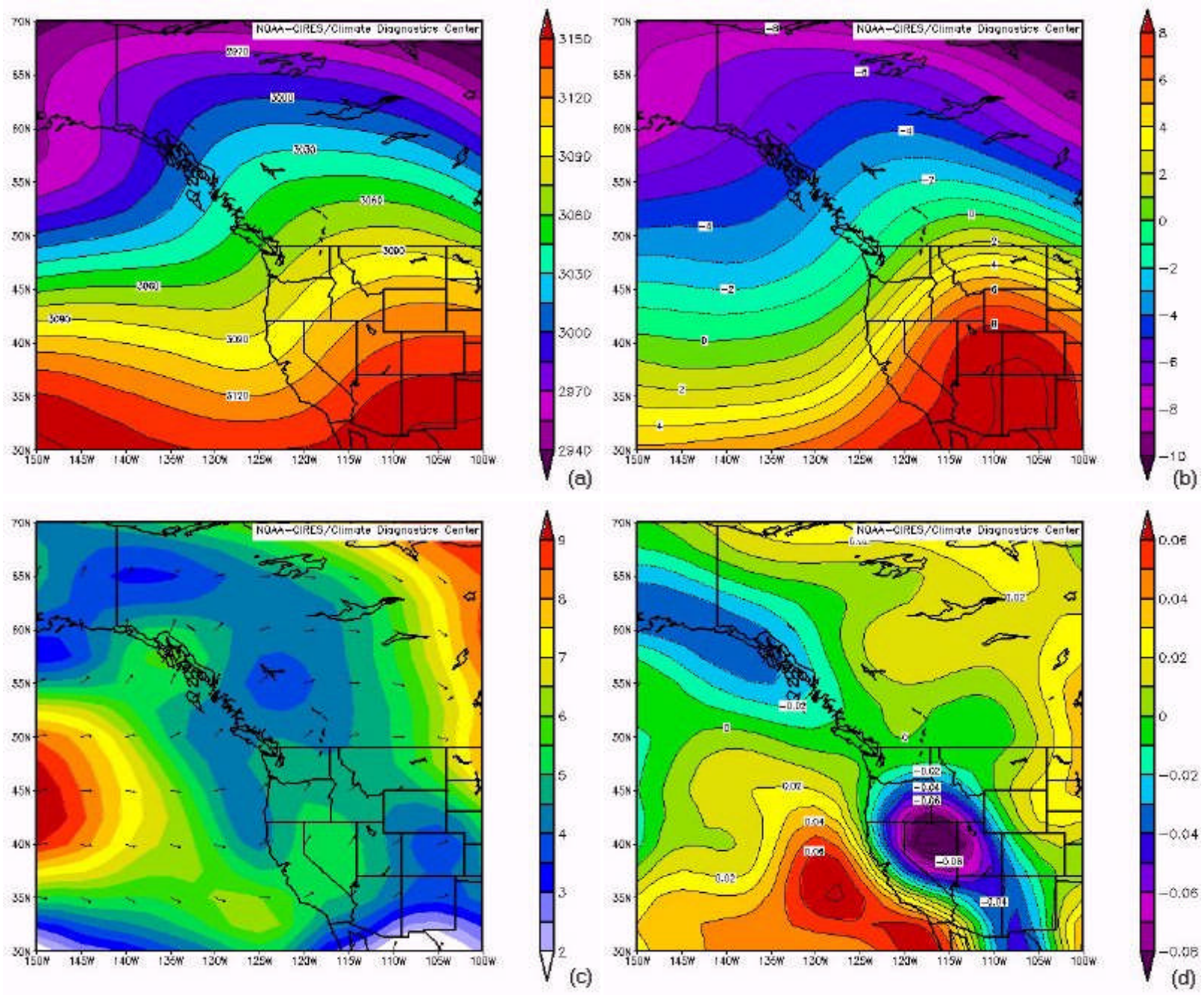

Figure 10: (a) Coastal Trough-Inland Ridge 700 mb height mean (m)
(b) Coastal Trough-Inland Ridge 700 mb temperature mean (^{o}C)
(c) Coastal Trough-Inland Ridge 700 mb wind speed mean (0.5 * m s^{-1})
(d) Coastal Trough-Inland Ridge 700 mb vertical velocity mean (Pascal s^{-1})

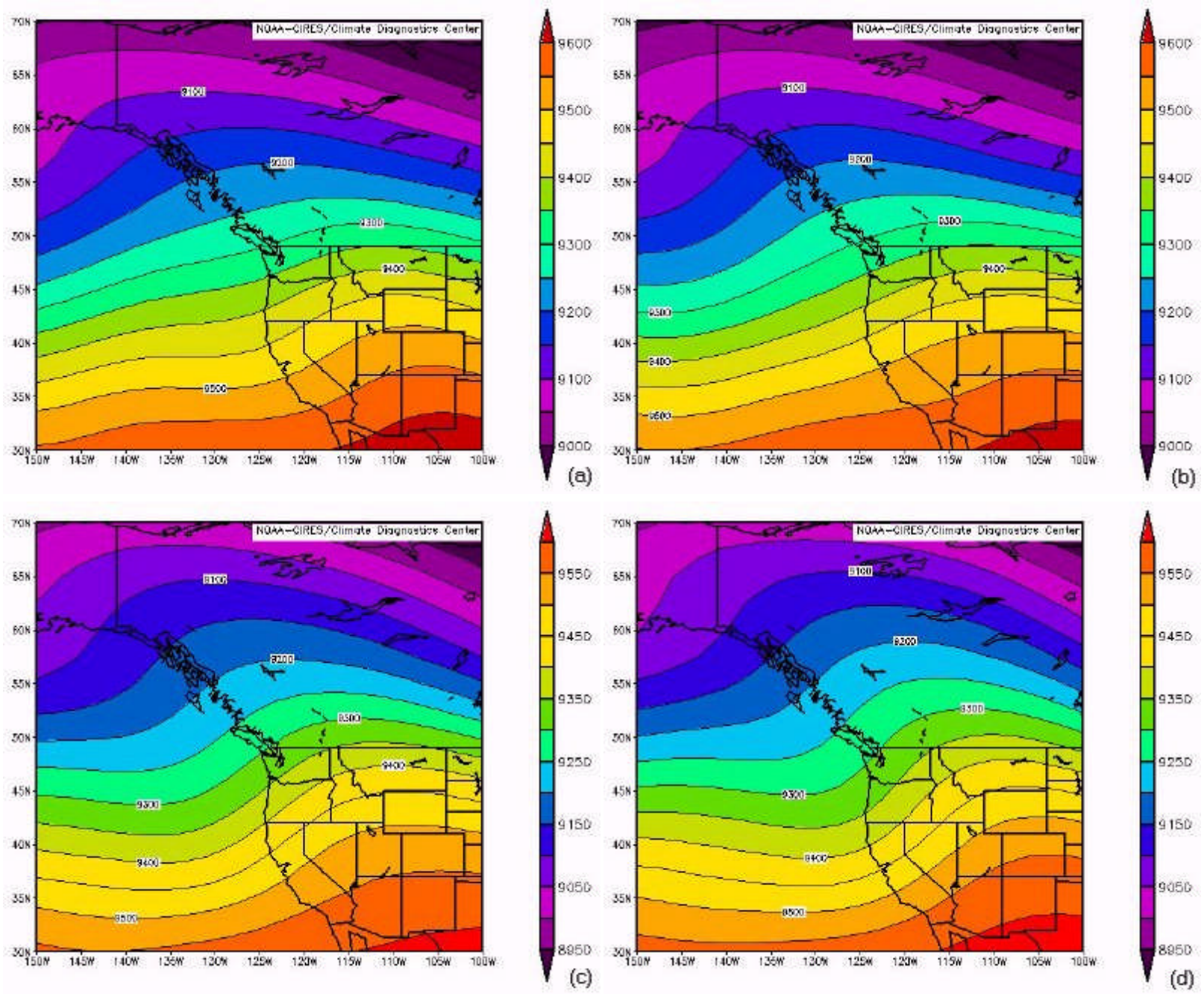

Figure 11: (a) Coastal Trough-Inland Ridge 300 mb height mean (D - 3) (m)
(b) Coastal Trough-Inland Ridge 300 mb height mean (D - 2) (m)
(c) Coastal Trough-Inland Ridge 300 mb height mean (D - 1) (m)
(d) Coastal Trough-Inland Ridge 300 mb height mean (D - 0) (m)

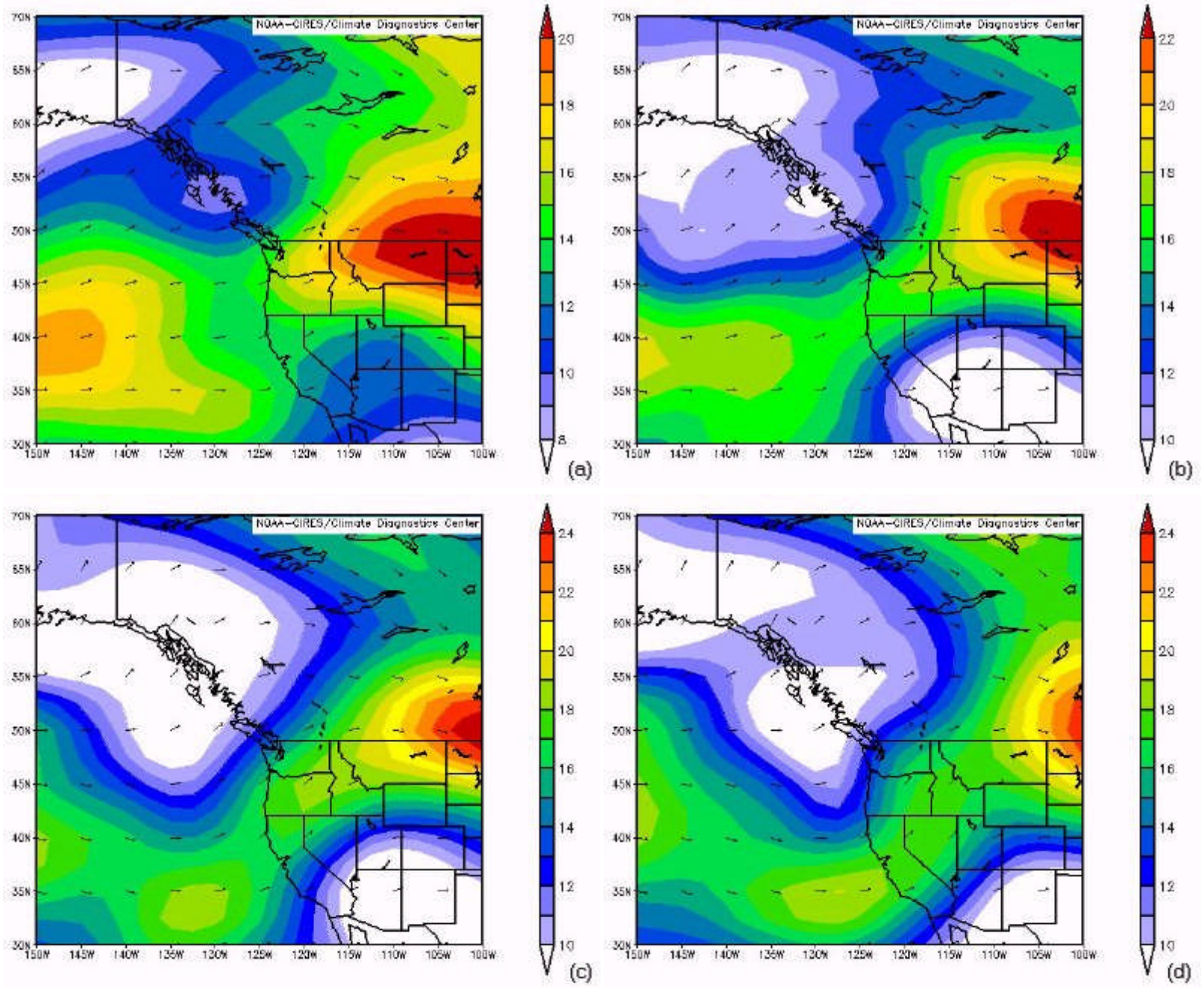

Figure 12: (a) Coastal Trough-Inland Ridge 300 mb wind speed mean (D - 3) (0.5 * m s^{-1})
(b) Coastal Trough-Inland Ridge 300 mb wind speed mean (D - 2) (0.5 * m s^{-1})
(c) Coastal Trough-Inland Ridge 300 mb wind speed mean (D - 1) (0.5 * m s^{-1})
(d) Coastal Trough-Inland Ridge 300 mb wind speed mean (D - 0) (0.5 * m s^{-1})

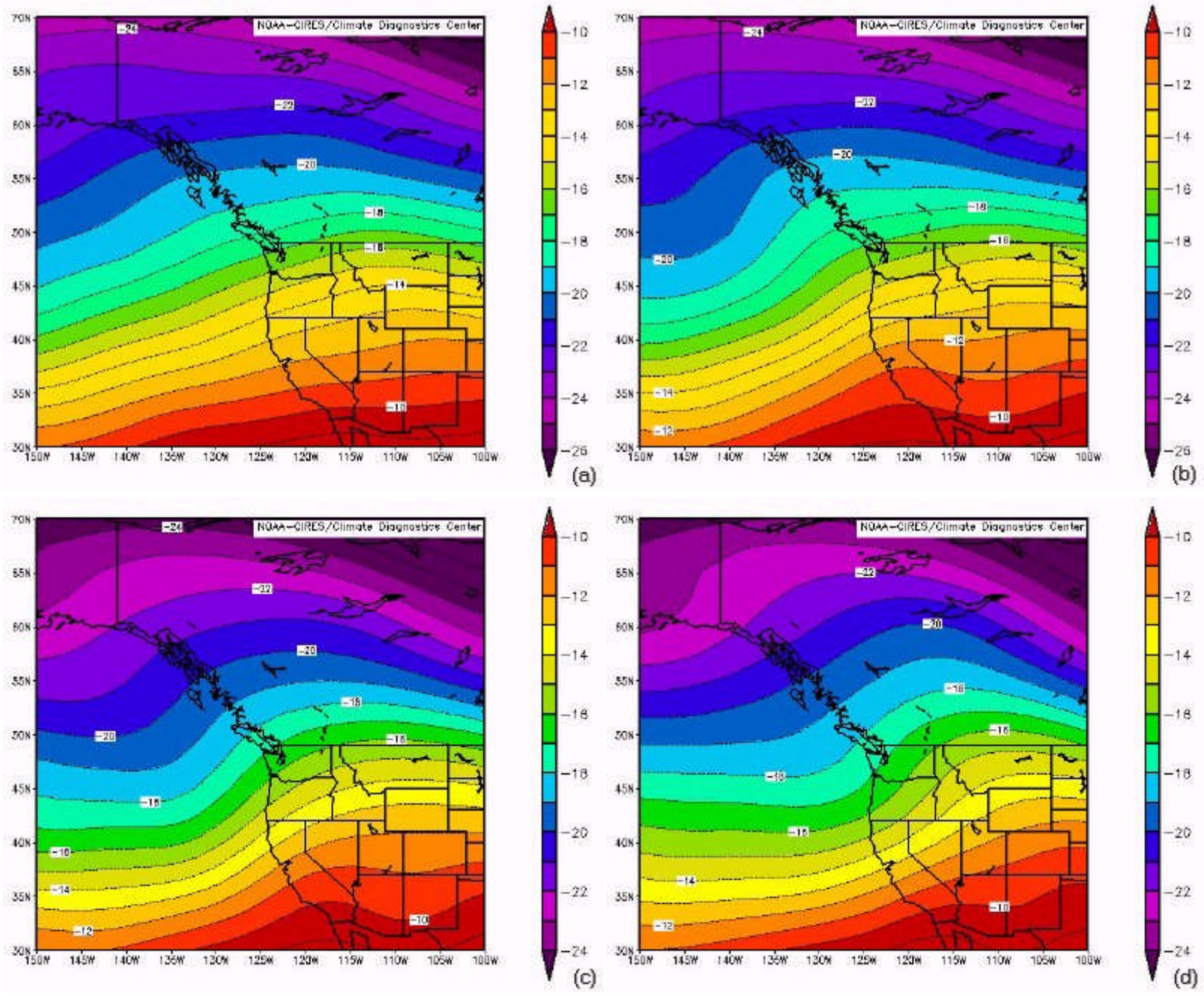

Figure 13: (a) Coastal Trough-Inland Ridge 500 mb temperature mean (D - 3) (^{o}C)
(b) Coastal Trough-Inland Ridge 500 mb temperature mean (D - 2) (^{o}C)
(c) Coastal Trough-Inland Ridge 500 mb temperature mean (D - 1) (^{o}C)
(d) Coastal Trough-Inland Ridge 500 mb temperature mean (D - 0) (^{o}C)

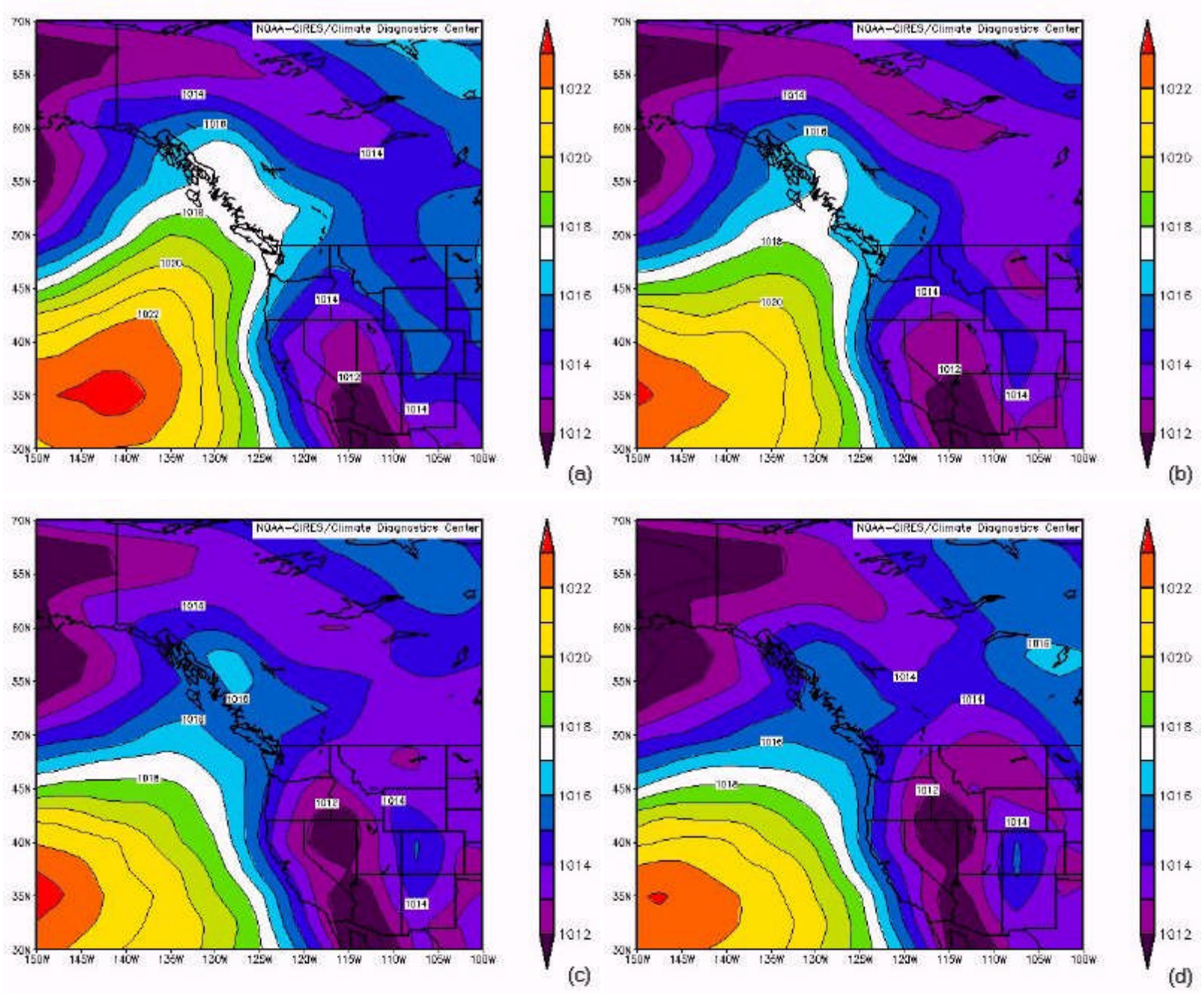

Figure 14: (a) Coastal Trough-Inland Ridge mean sea-level pressure mean (D - 3) (mb)
(b) Coastal Trough-Inland Ridge mean sea-level pressure mean (D - 2) (mb)
(c) Coastal Trough-Inland Ridge mean sea-level pressure mean (D - 1) (mb)
(d) Coastal Trough-Inland Ridge mean sea-level pressure mean (D - 0) (mb)

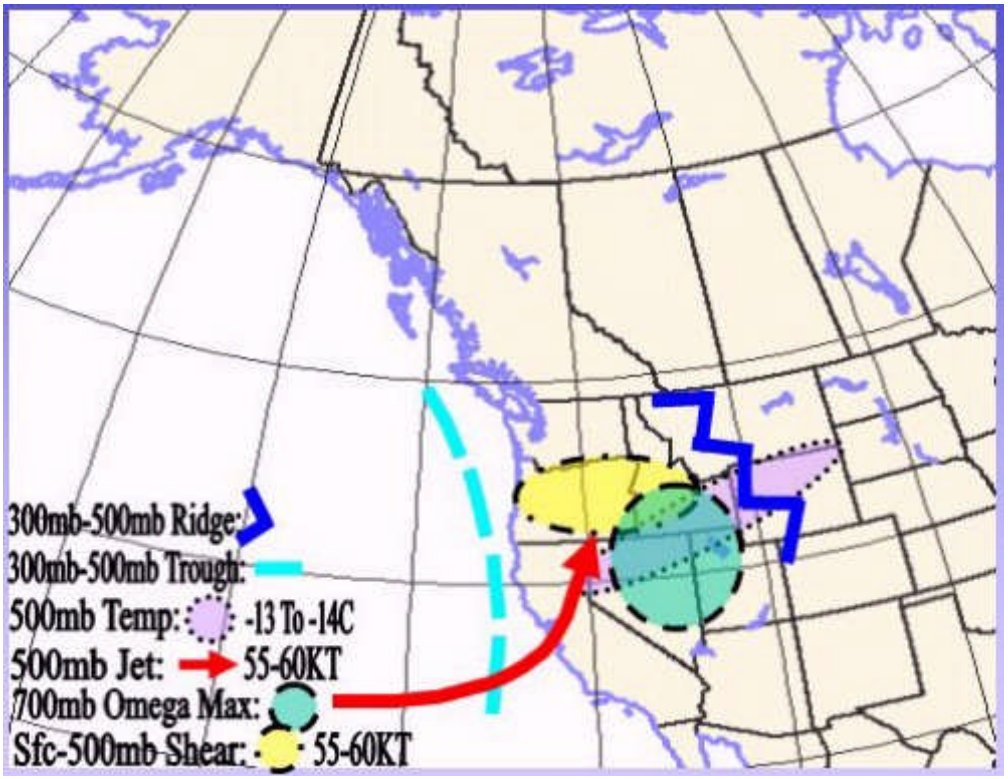

Figure 15: Coastal Trough-Inland Ridge Composite Synoptic Pattern

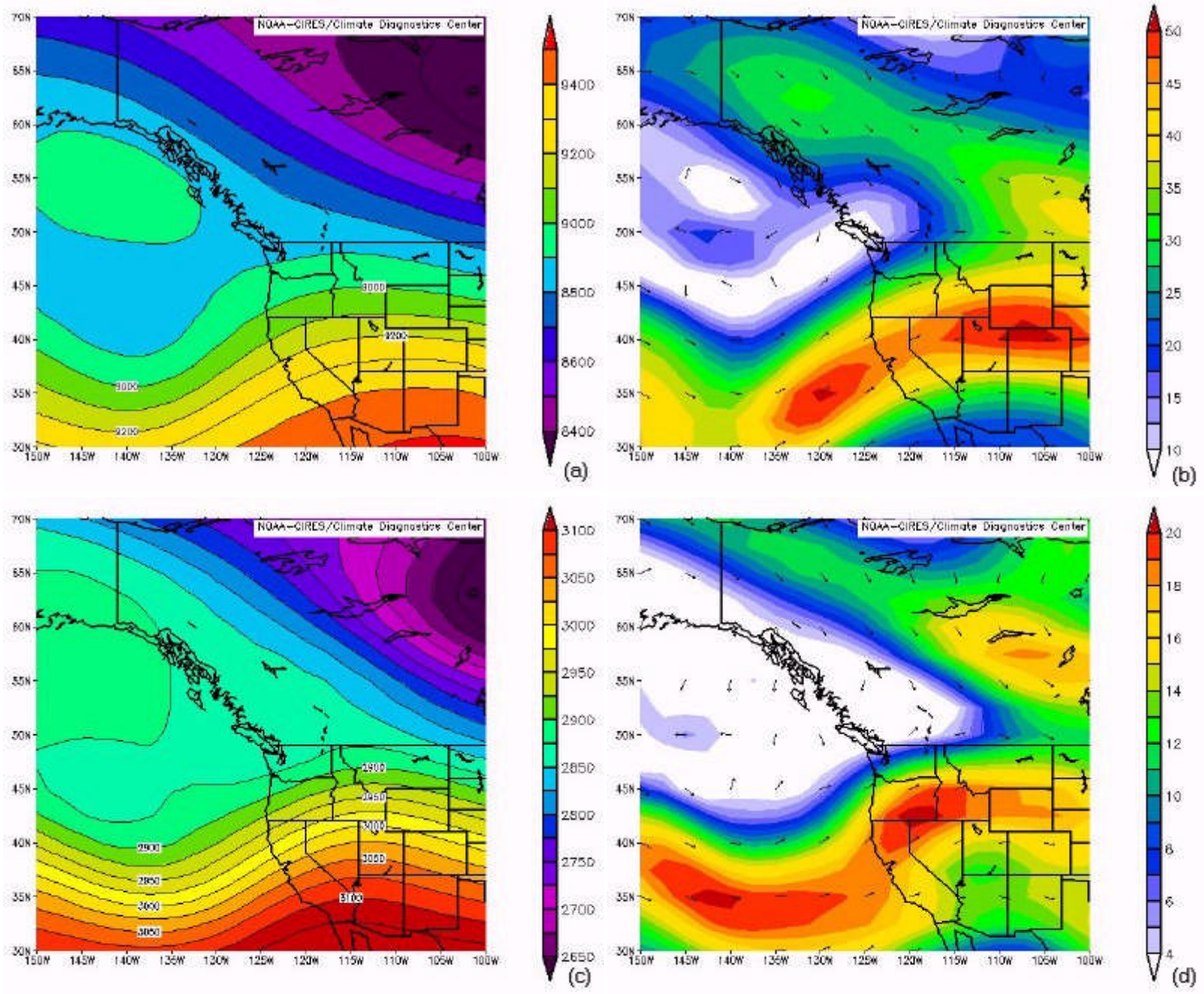

Figure 16: (a) Coastal Trough-Inland Ridge 300 mb height (m): 2000 February 14-15
(b) Coastal Trough-Inland Ridge 300 mb wind speed (m s^{-1}): 2000 February 14-15
(c) Coastal Trough-Inland Ridge 700 mb height (m): 2000 February 14-15
(d) Coastal Trough-Inland Ridge 700 mb wind speed (m s^{-1}): 2000 February 14-15

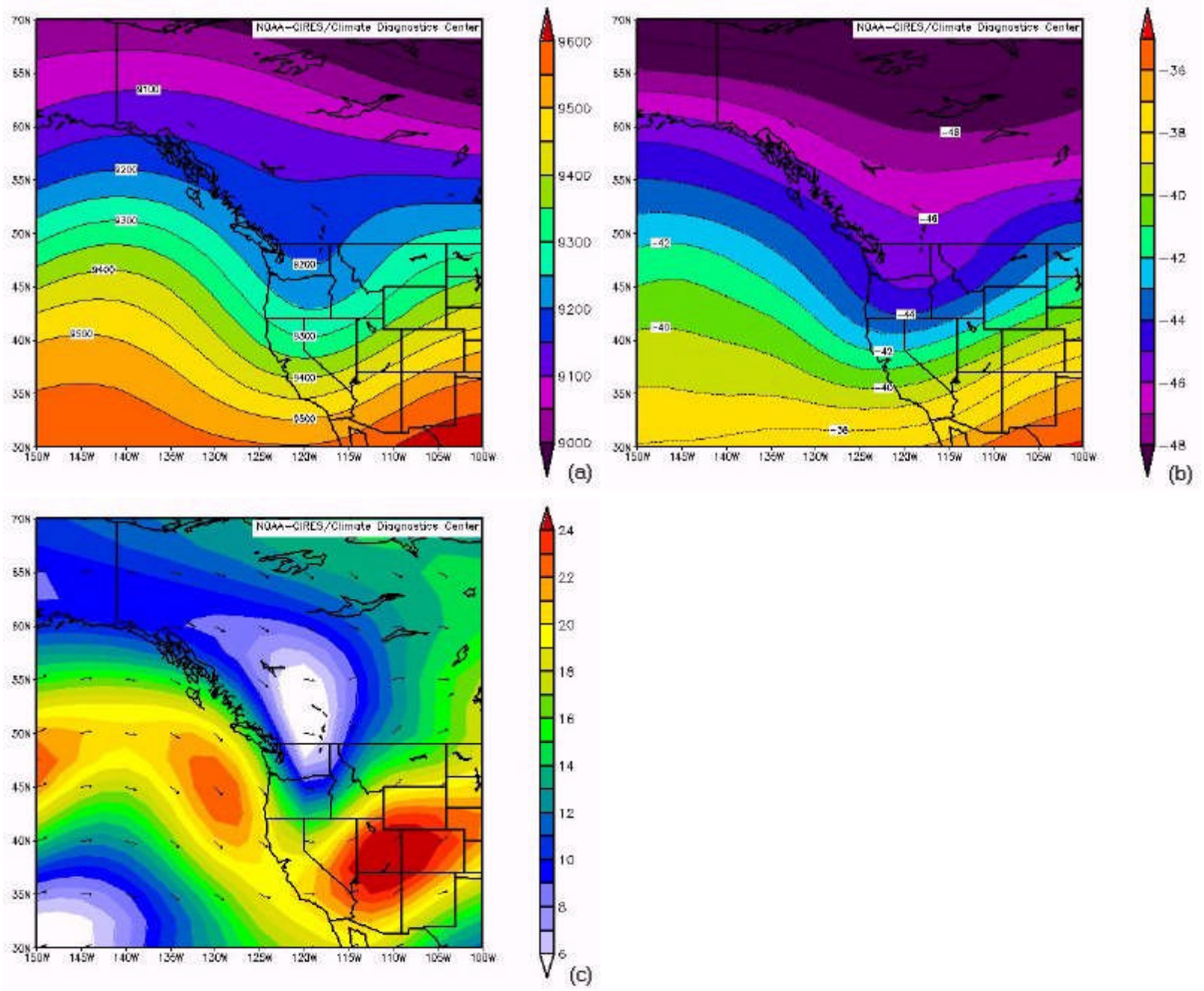

Figure 17: (a) Coastal Ridge-Inland Trough 300 mb height mean (m)

(b) Coastal Ridge-Inland Trough 300 mb temperature mean (^{o}C)

(c) Coastal Ridge-Inland Trough 300 mb wind speed mean (0.5 * m s^{-1})

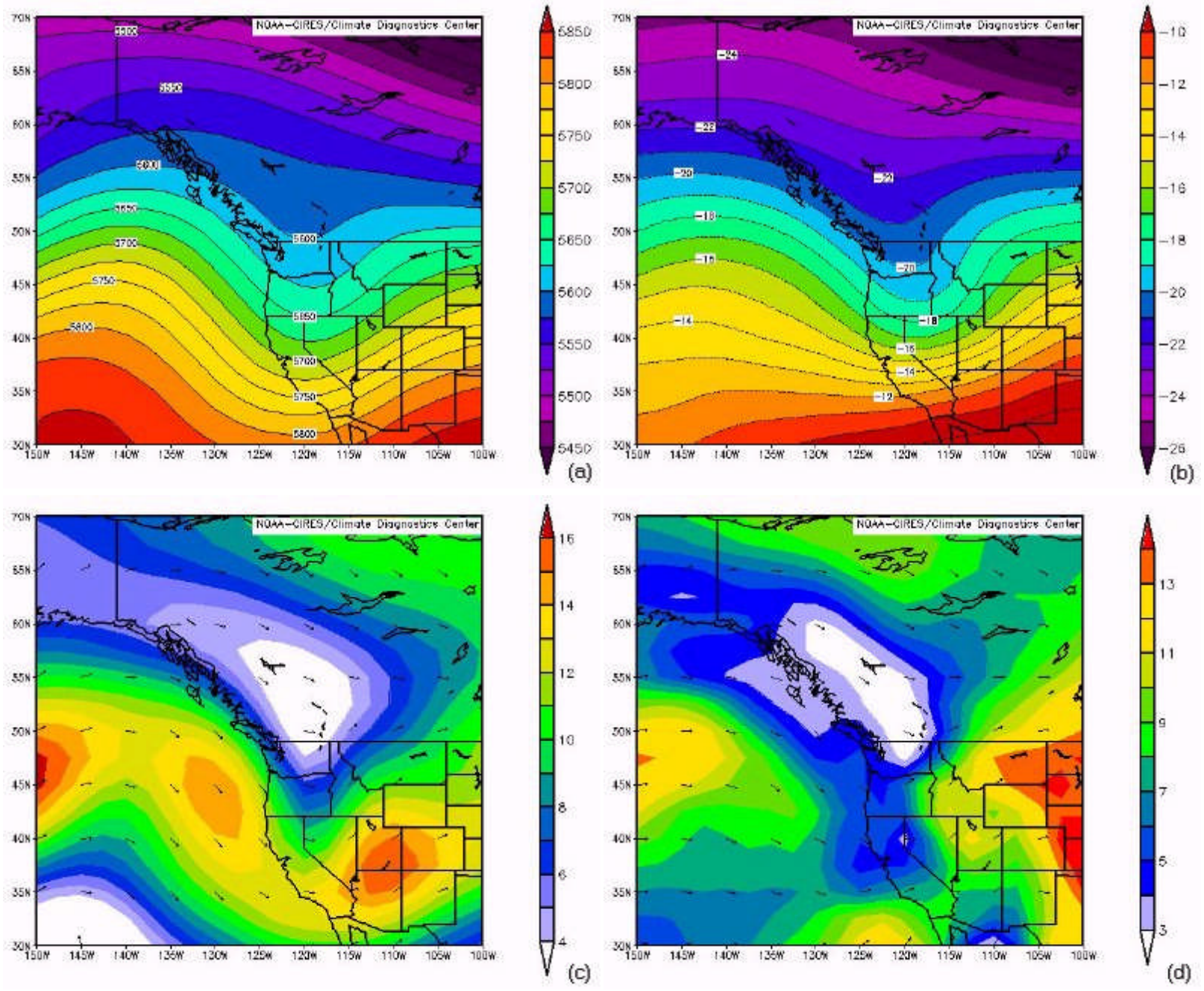

Figure 18: (a) Coastal Ridge-Inland Trough 500 mb height mean (m)
(b) Coastal Ridge-Inland Trough 500 mb temperature mean (^{o}C)
(c) Coastal Ridge-Inland Trough 500 mb wind speed mean (0.5 * m s^{-1})
(d) Coastal Ridge-Inland Trough surface to 500 mb wind shear mean (0.5 * m s^{-1})

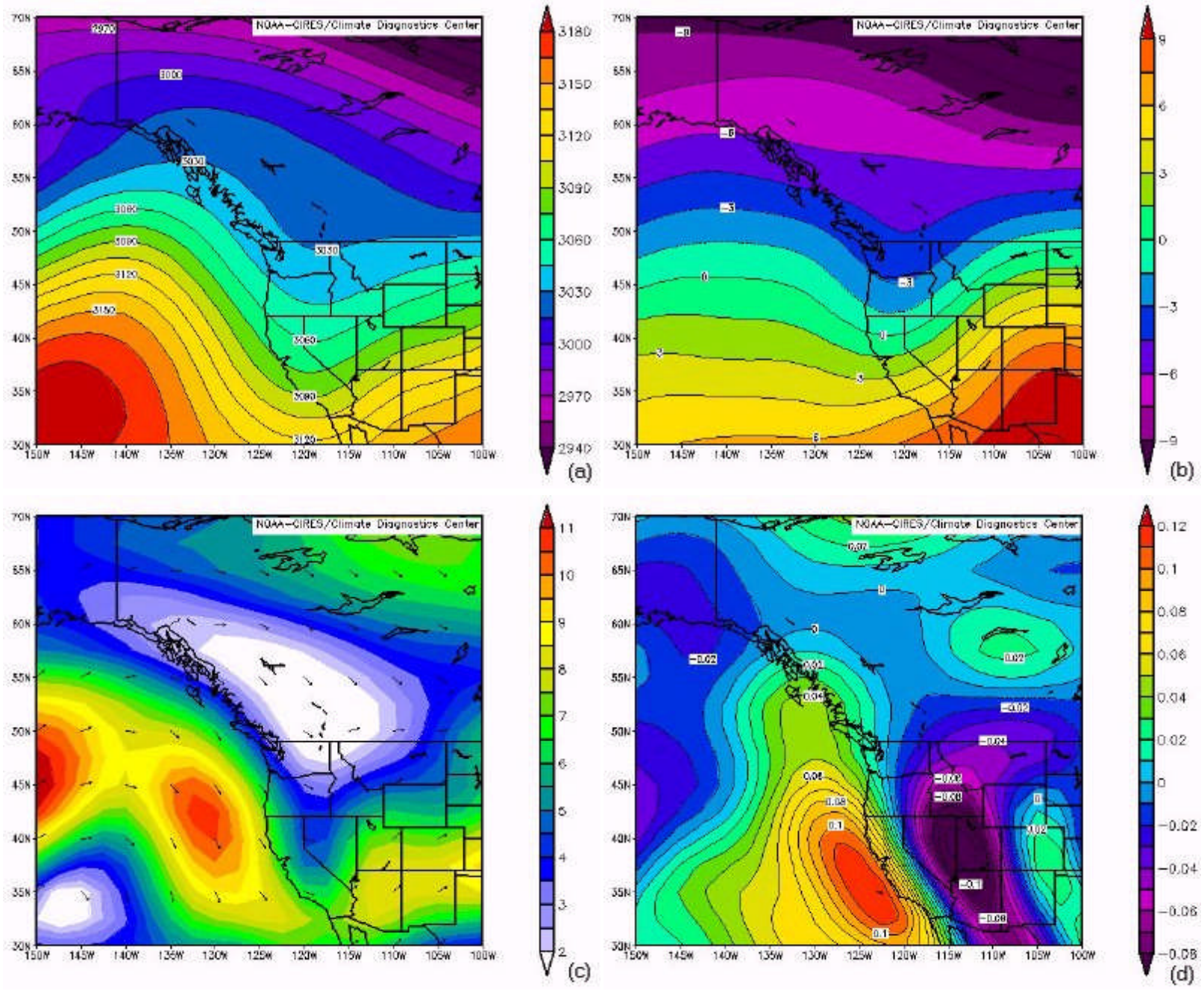

Figure 19: (a) Coastal Ridge-Inland Trough 700 mb height mean (m)
(b) Coastal Ridge-Inland Trough 700 mb temperature mean (^{o}C)
(c) Coastal Ridge-Inland Trough 700 mb wind speed mean (0.5 * m s^{-1})
(d) Coastal Ridge-Inland Trough 700 mb vertical velocity mean (Pascal s^{-1})

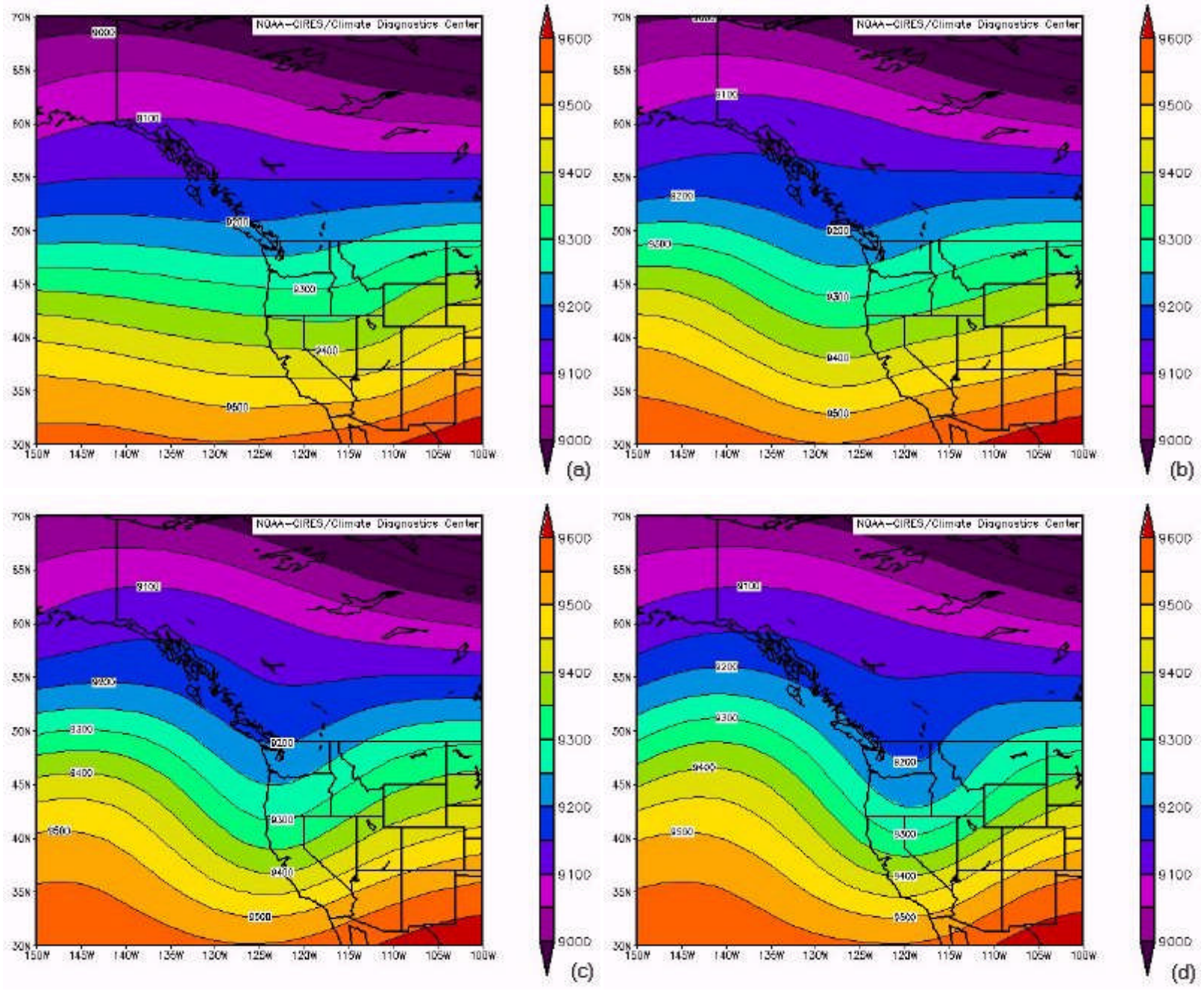

Figure 20: (a) Coastal Ridge-Inland Trough 300 mb height mean (D - 3) (m)
(b) Coastal Ridge-Inland Trough 300 mb height mean (D - 2) (m)
(c) Coastal Ridge-Inland Trough 300 mb height mean (D - 1) (m)
(d) Coastal Ridge-Inland Trough 300 mb height mean (D - 0) (m)

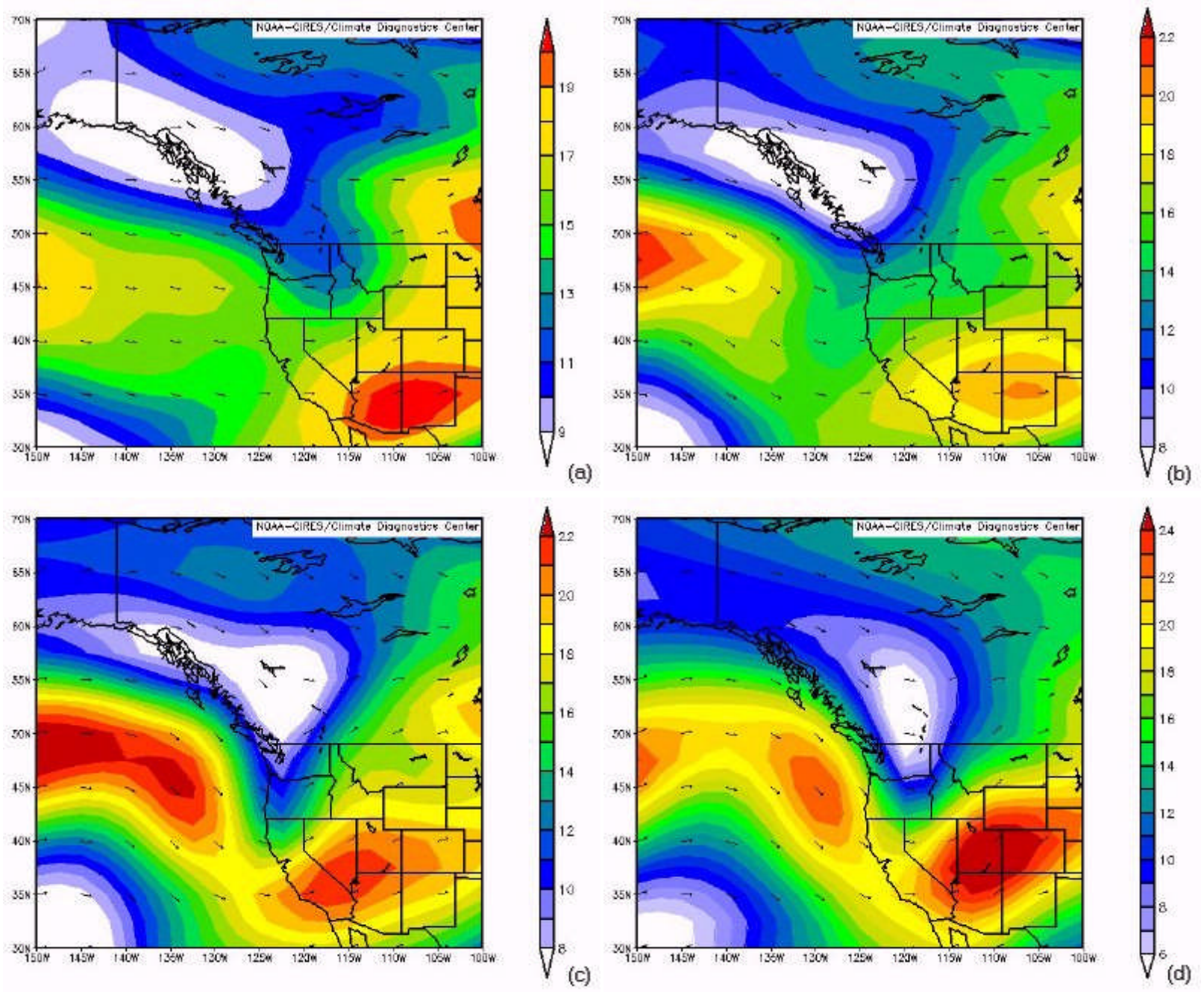

Figure 21: (a) Coastal Ridge-Inland Trough 300 mb wind speed mean (D - 3) (0.5 * m s^{-1})
(b) Coastal Ridge-Inland Trough 300 mb wind speed mean (D - 2) (0.5 * m s^{-1})
(c) Coastal Ridge-Inland Trough 300 mb wind speed mean (D - 1) (0.5 * m s^{-1})
(d) Coastal Ridge-Inland Trough 300 mb wind speed mean (D - 0) (0.5 * m s^{-1})

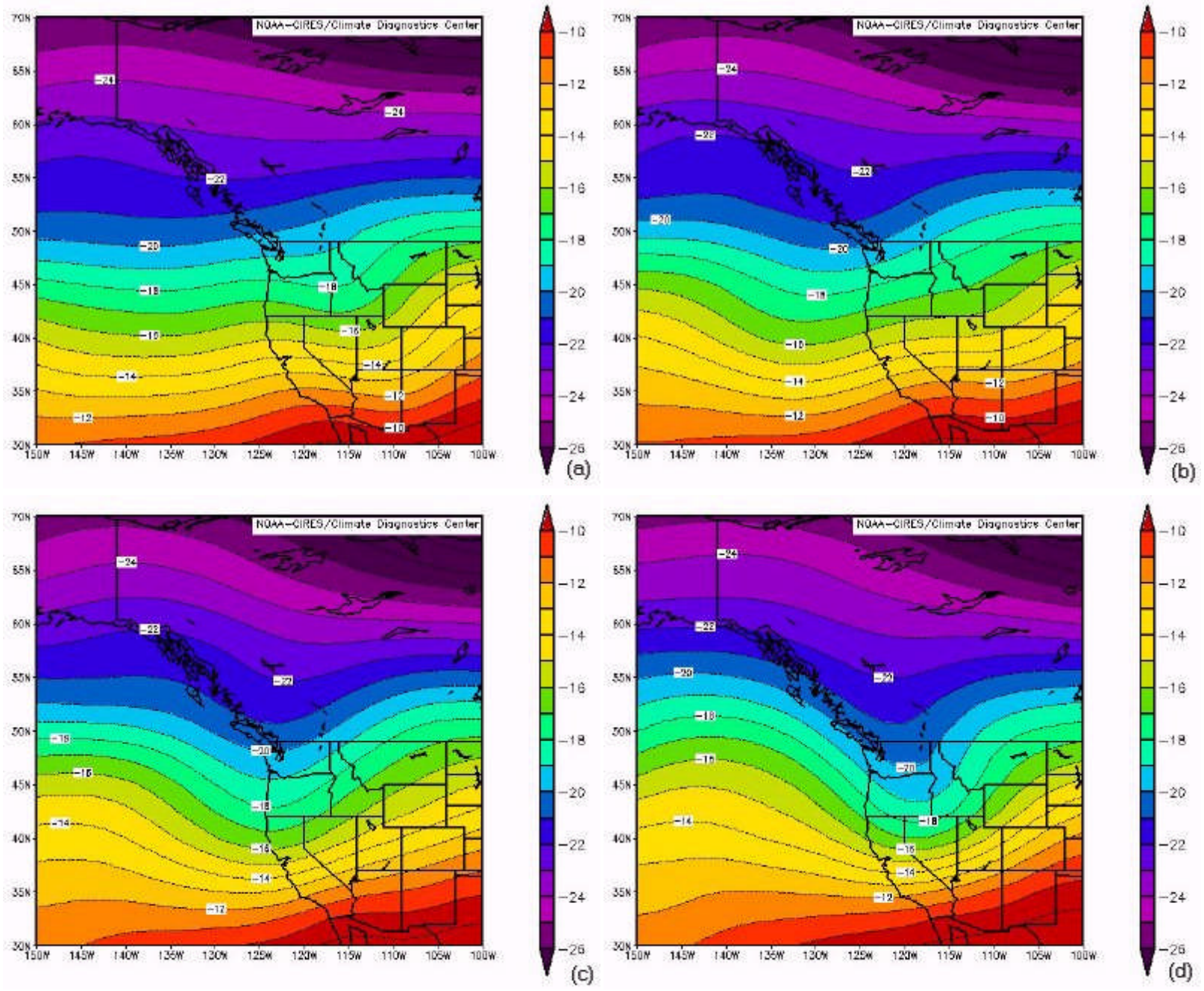

Figure 22: (a) Coastal Ridge-Inland Trough 500 mb temperature mean (D - 3) (^{o}C)
(b) Coastal Ridge-Inland Trough 500 mb temperature mean (D - 2) (^{o}C)
(c) Coastal Ridge-Inland Trough 500 mb temperature mean (D - 1) (^{o}C)
(d) Coastal Ridge-Inland Trough 500 mb temperature mean (D - 0) (^{o}C)

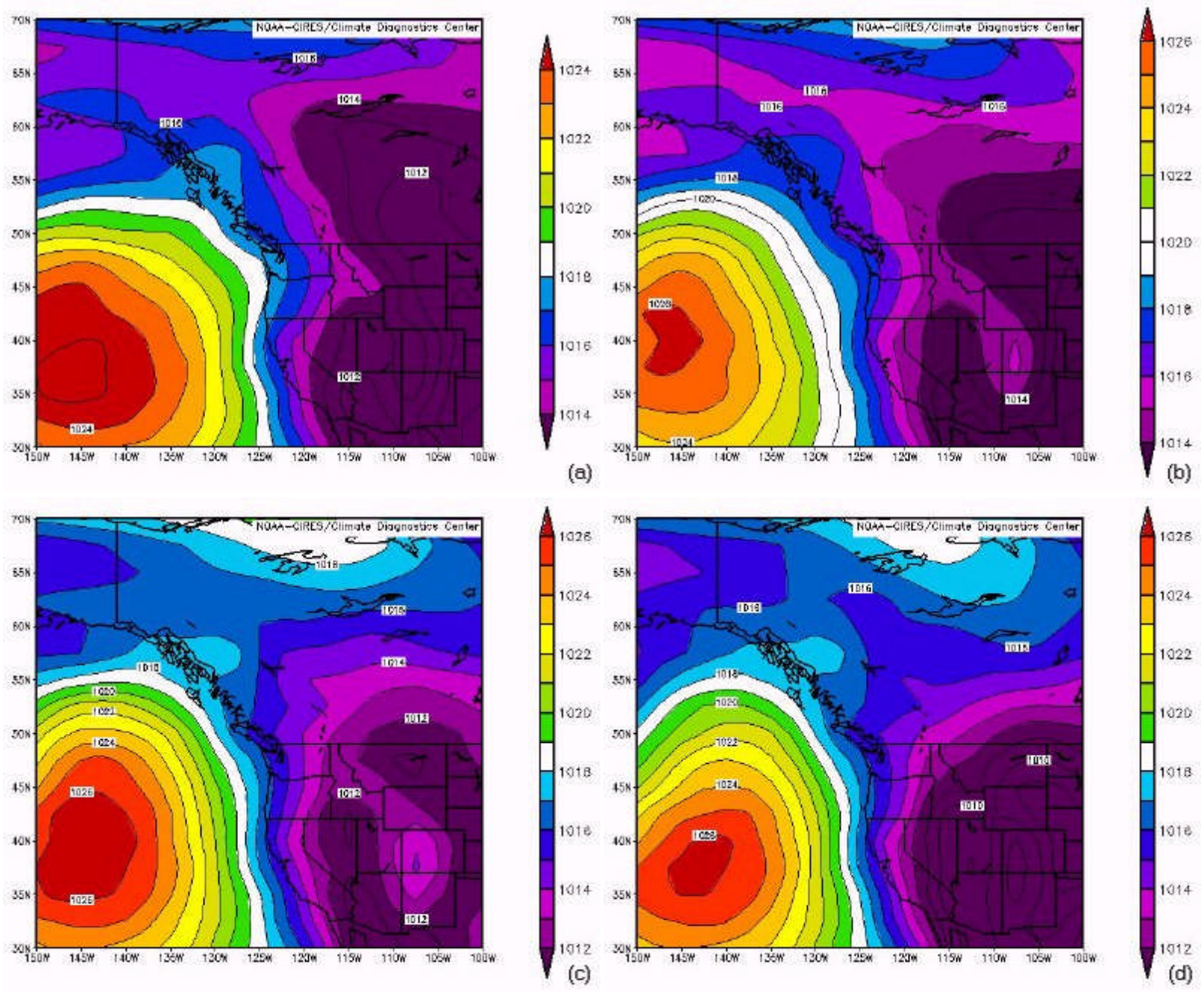

Figure 23: (a) Coastal Ridge-Inland Trough mean sea-level pressure mean (D - 3) (mb)
(b) Coastal Ridge-Inland Trough mean sea-level pressure mean (D - 2) (mb)
(c) Coastal Ridge-Inland Trough mean sea-level pressure mean (D - 1) (mb)
(d) Coastal Ridge-Inland Trough mean sea-level pressure mean (D - 0) (mb)

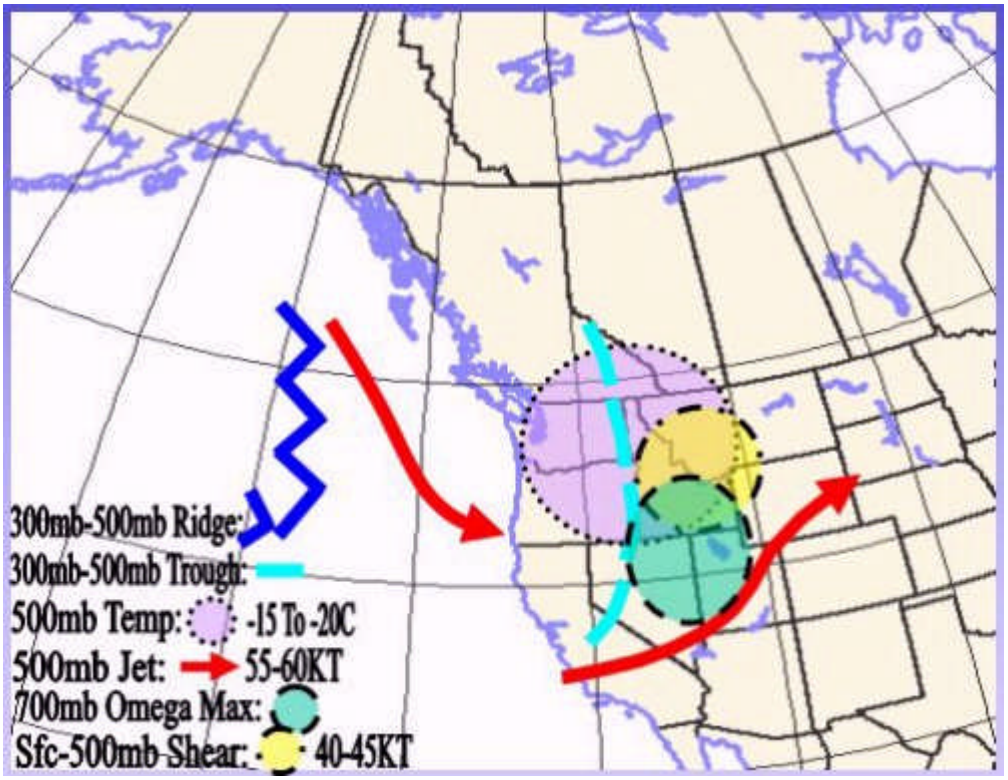

Figure 24: Coastal Ridge-Inland Trough Composite Synoptic Pattern

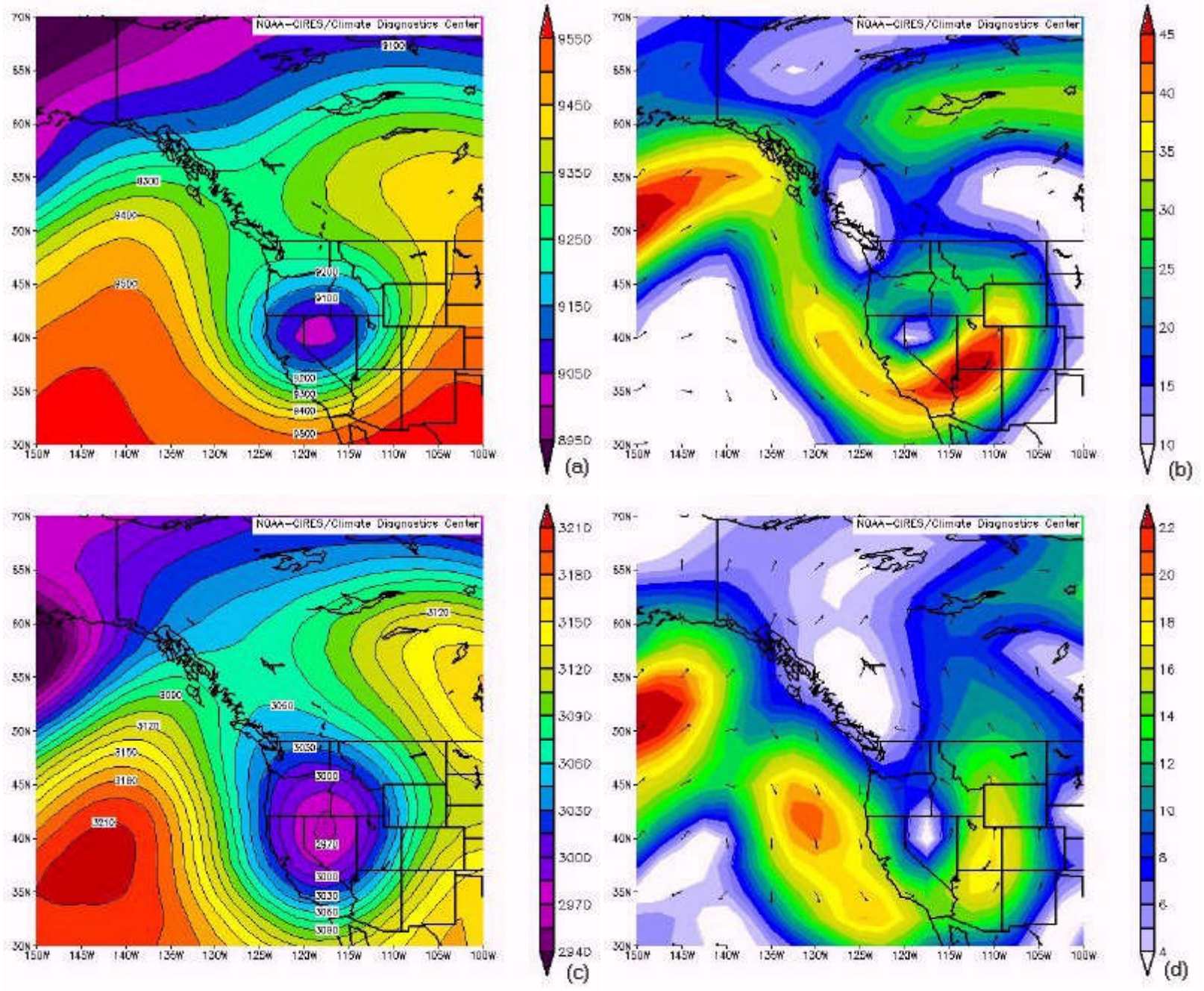

Figure 25: (a) Coastal Ridge-Inland Trough 300 mb height (m): 1991 May 18
(b) Coastal Ridge-Inland Trough 300 mb wind speed (m s^{-1}): 1991 May 18
(c) Coastal Ridge-Inland Trough 700 mb height (m): 1991 May 18
(d) Coastal Ridge-Inland Trough 700 mb wind speed (m s^{-1}): 1991 May 18

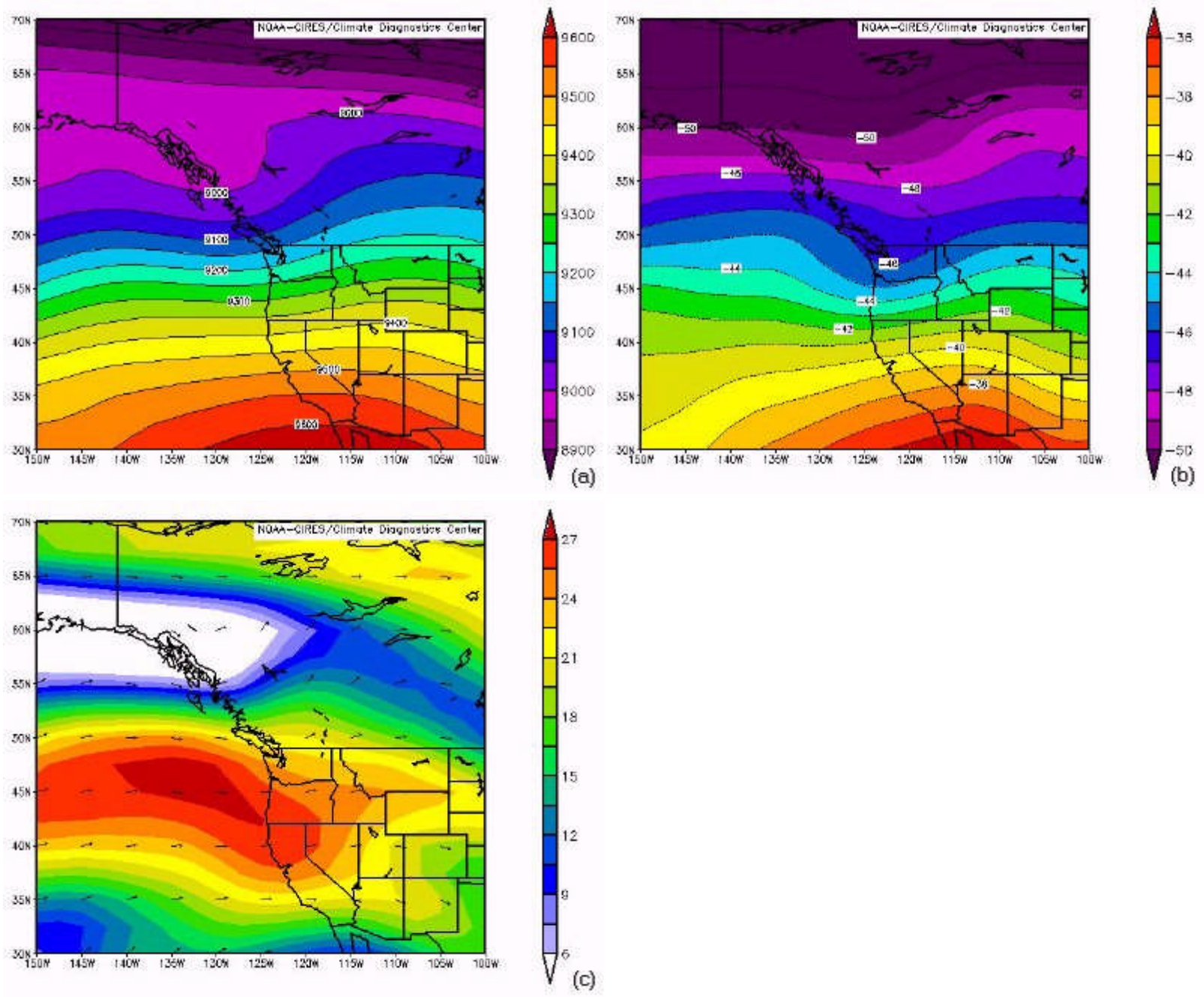

Figure 26: (a) Zonal 300 mb height mean (m)
(b) Zonal 300 mb temperature mean (^{o}C)
(c) Zonal 300 mb wind speed mean (0.5 * m s^{-1})

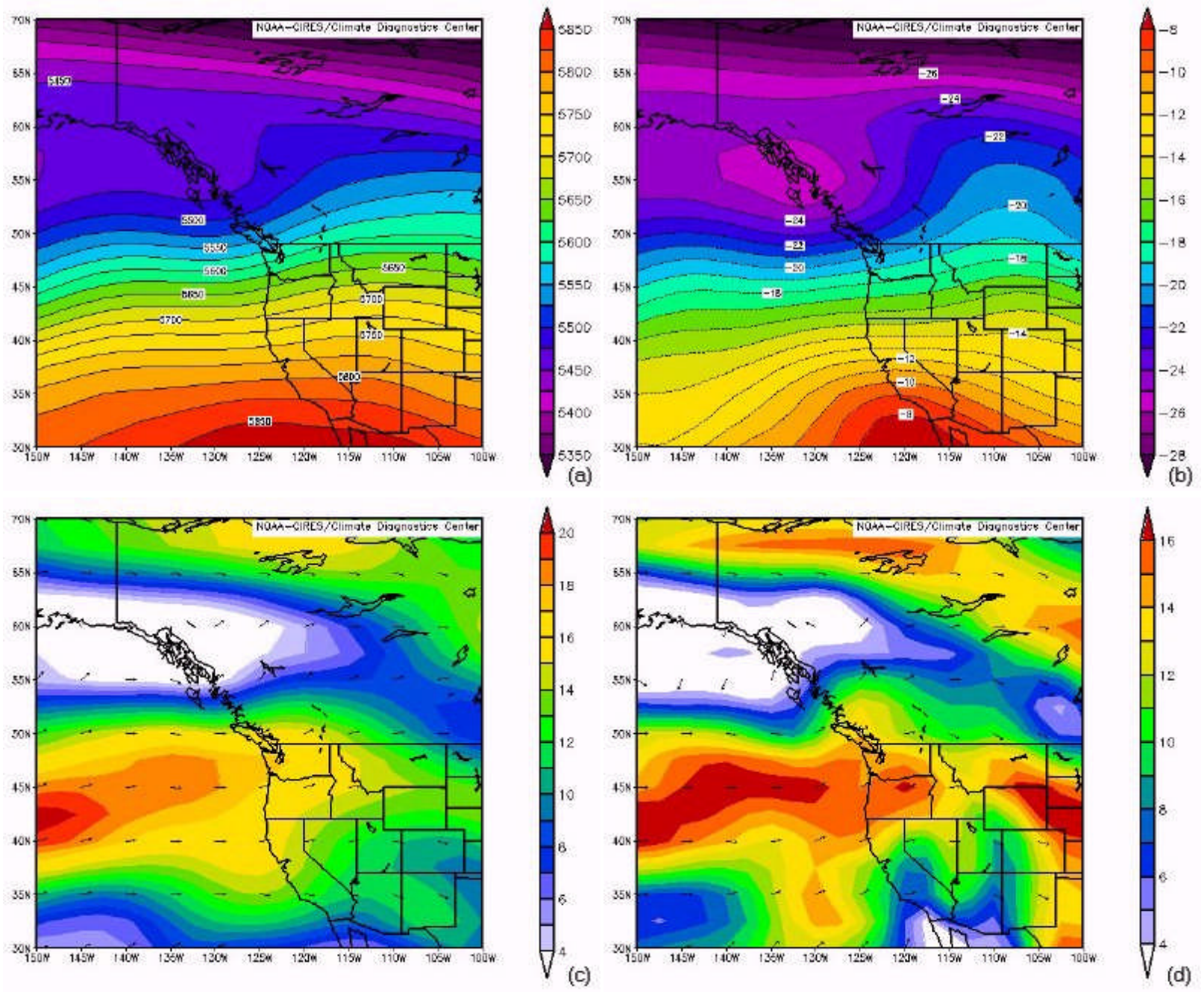

Figure 27: (a) Zonal 500 mb height mean (m)
(b) Zonal 500 mb temperature mean (^{o}C)
(c) Zonal 500 mb wind speed mean (0.5 * m s^{-1})
(d) Zonal surface to 500 mb wind shear mean (0.5 * m s^{-1})

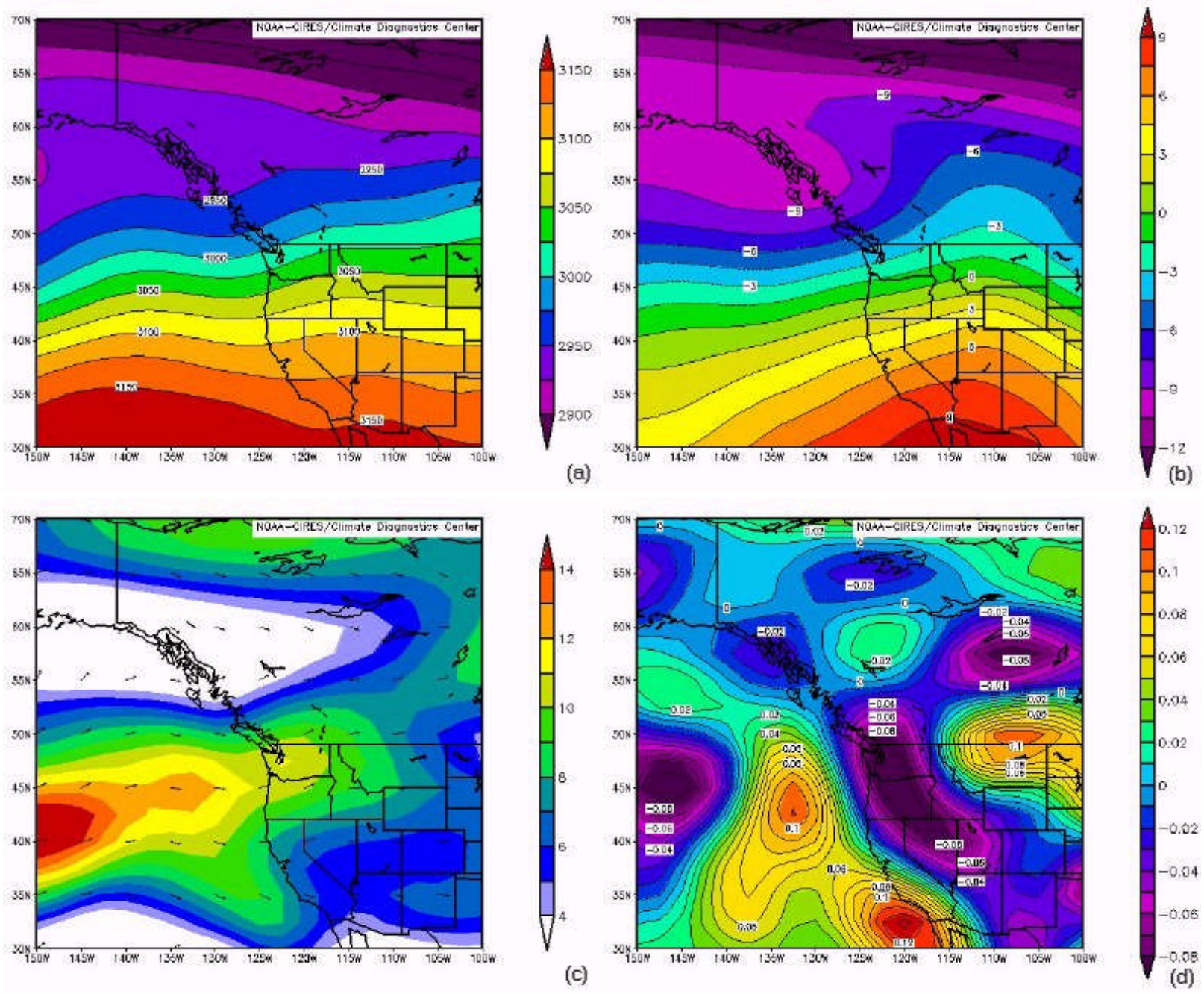

Figure 28: (a) Zonal 700 mb height mean (m)
(b) Zonal 700 mb temperature mean (^{o}C)
(c) Zonal 700 mb wind speed mean (0.5 * m s^{-1})
(d) Zonal 700 mb vertical velocity mean (Pascal s^{-1})

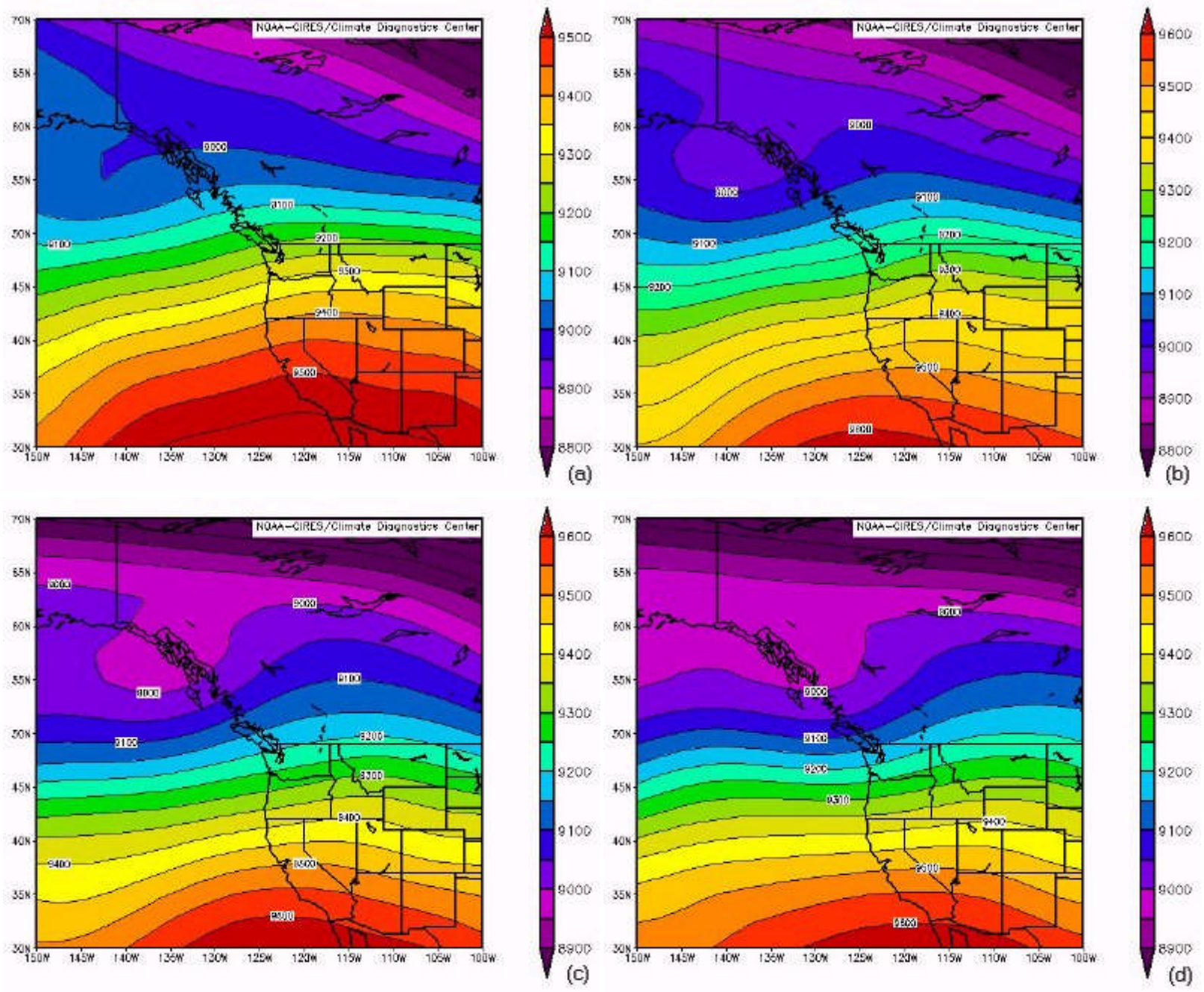

Figure 29: (a) Zonal 300 mb height mean (D - 3) (m)
(b) Zonal 300 mb height mean (D - 2) (m)
(c) Zonal 300 mb height mean (D - 1) (m)
(d) Zonal 300 mb height mean (D - 0) (m)

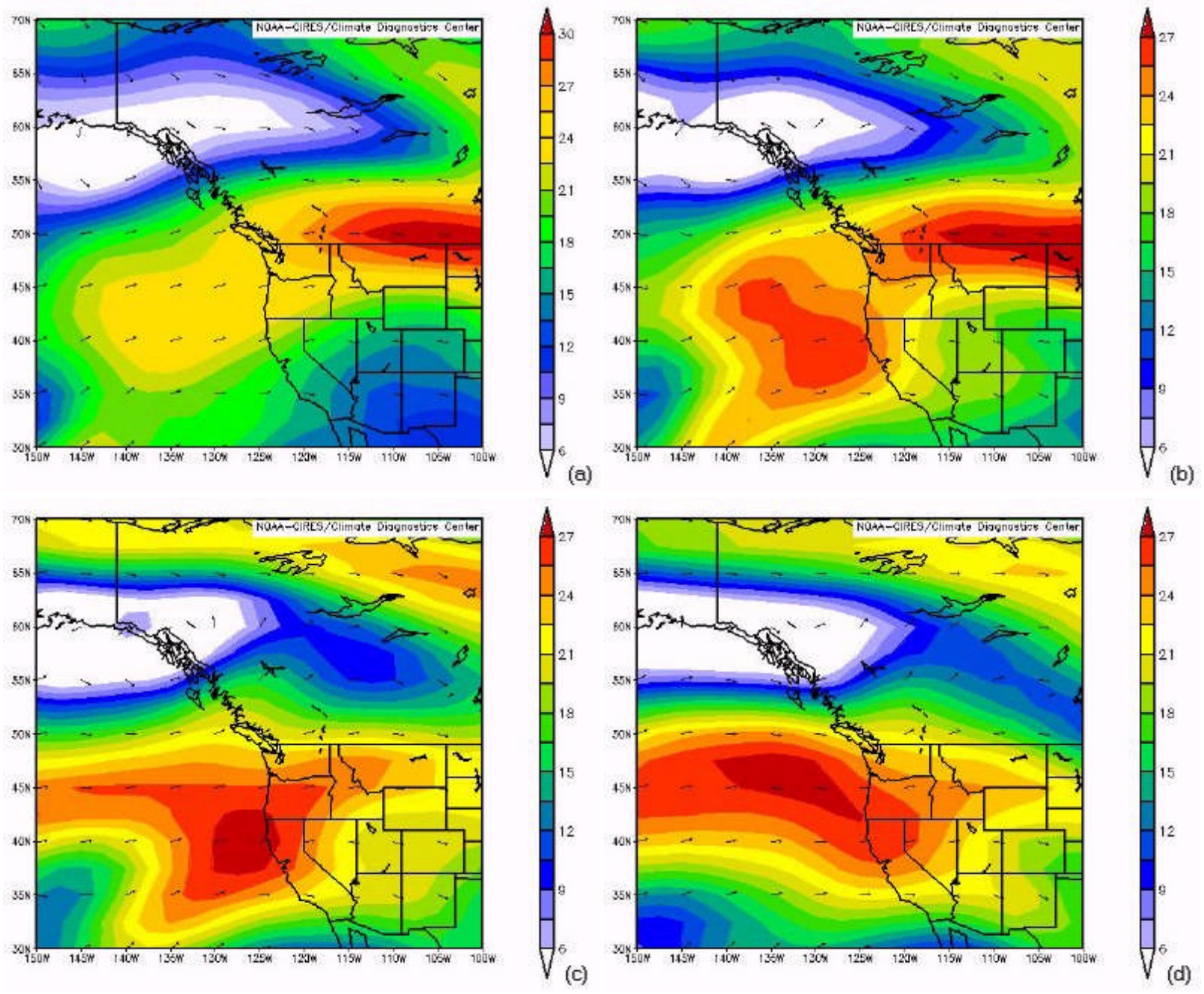

Figure 30: (a) Zonal 300 mb wind speed mean (D - 3) (0.5 * m s^{-1})
(b) Zonal 300 mb wind speed mean (D - 2) (0.5 * m s^{-1})
(c) Zonal 300 mb wind speed mean (D - 1) (0.5 * m s^{-1})
(d) Zonal 300 mb wind speed mean (D - 0) (0.5 * m s^{-1})

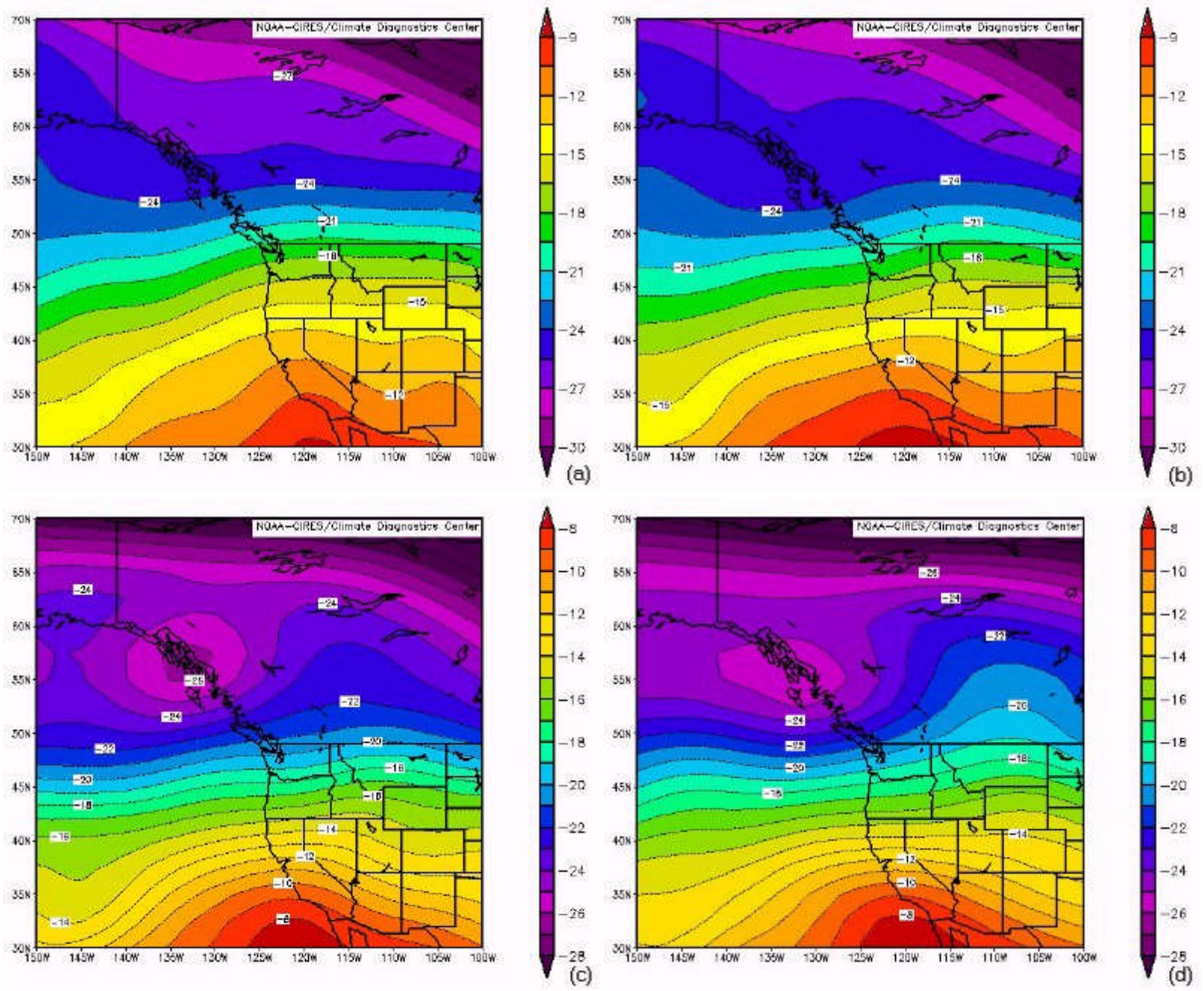

Figure 31: (a) Zonal 500 mb temperature mean (D - 3) (^{o}C)
(b) Zonal 500 mb temperature mean (D - 2) (^{o}C)
(c) Zonal 500 mb temperature mean (D - 1) (^{o}C)
(d) Zonal 500 mb temperature mean (D - 0) (^{o}C)

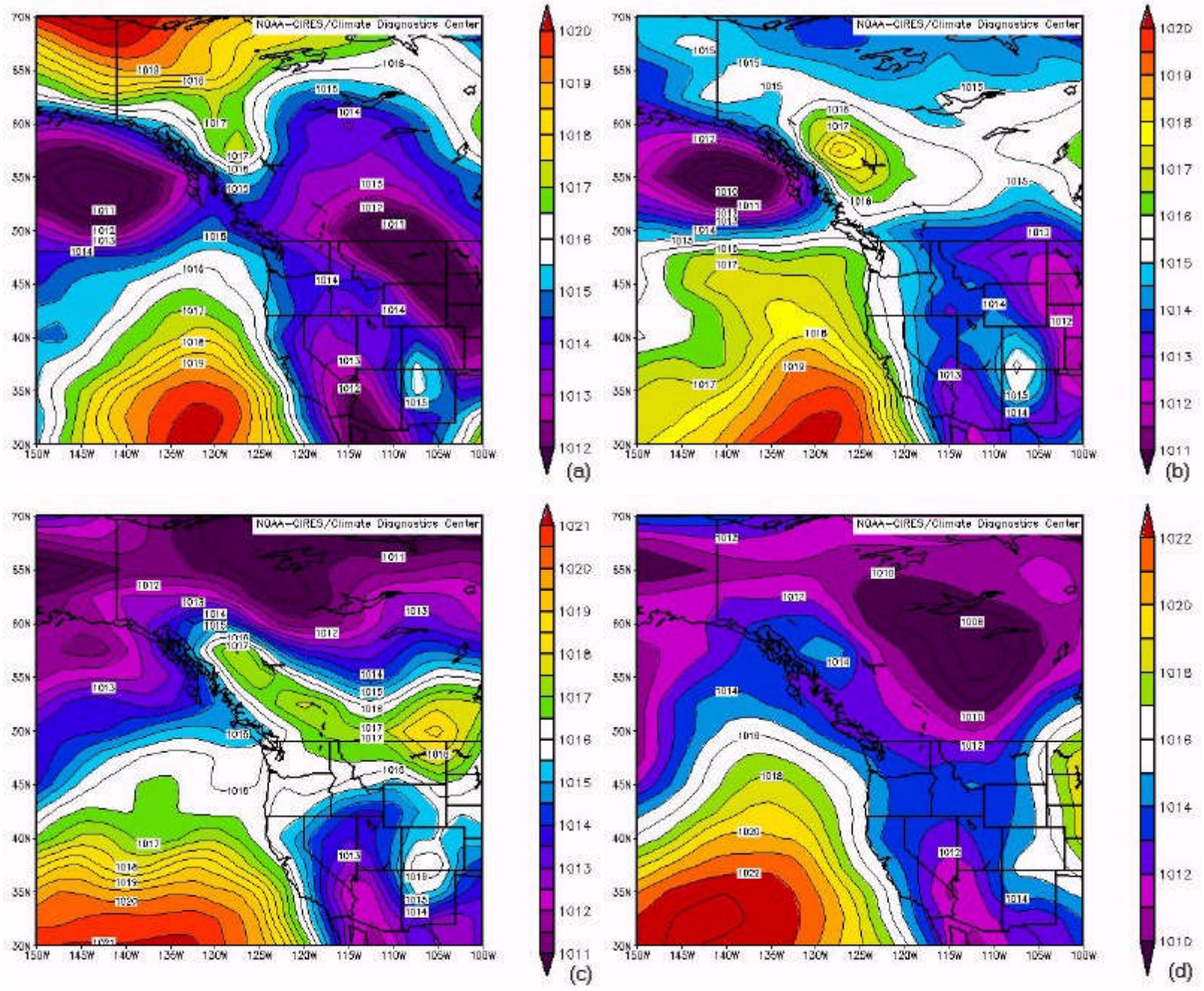

Figure 32: (a) Zonal mean sea-level pressure mean (D - 3) (mb)
(b) Zonal mean sea-level pressure mean (D - 2) (mb)
(c) Zonal mean sea-level pressure mean (D - 1) (mb)
(d) Zonal mean sea-level pressure mean (D - 0) (mb)

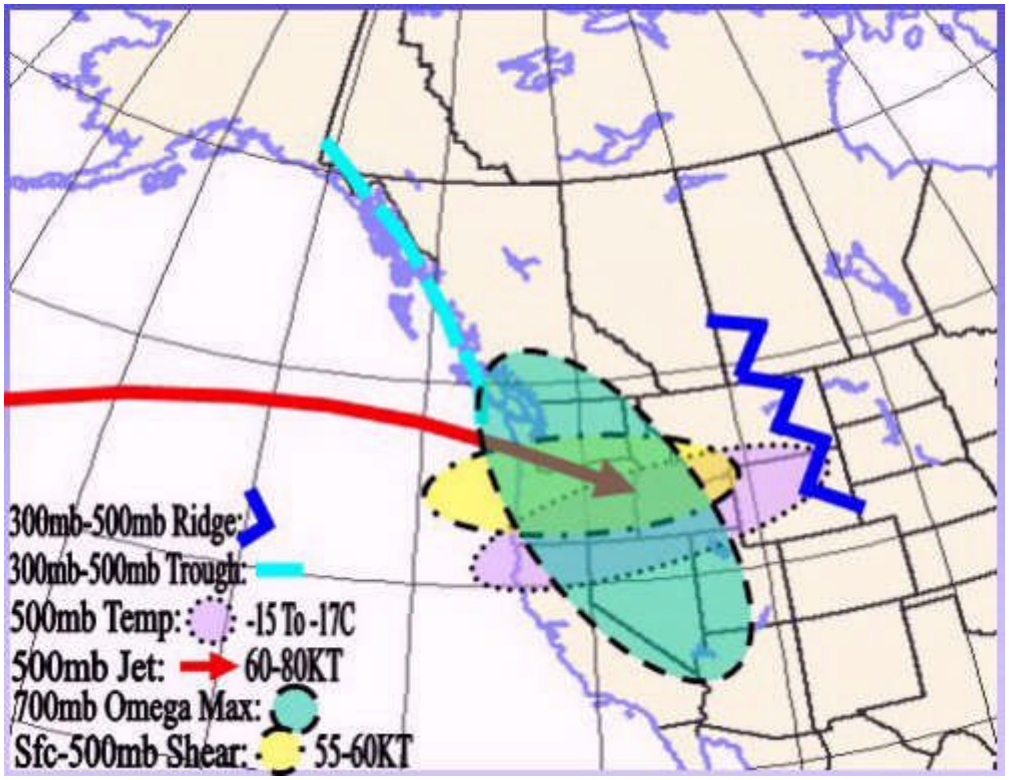

Figure 33: Zonal Composite Synoptic Pattern

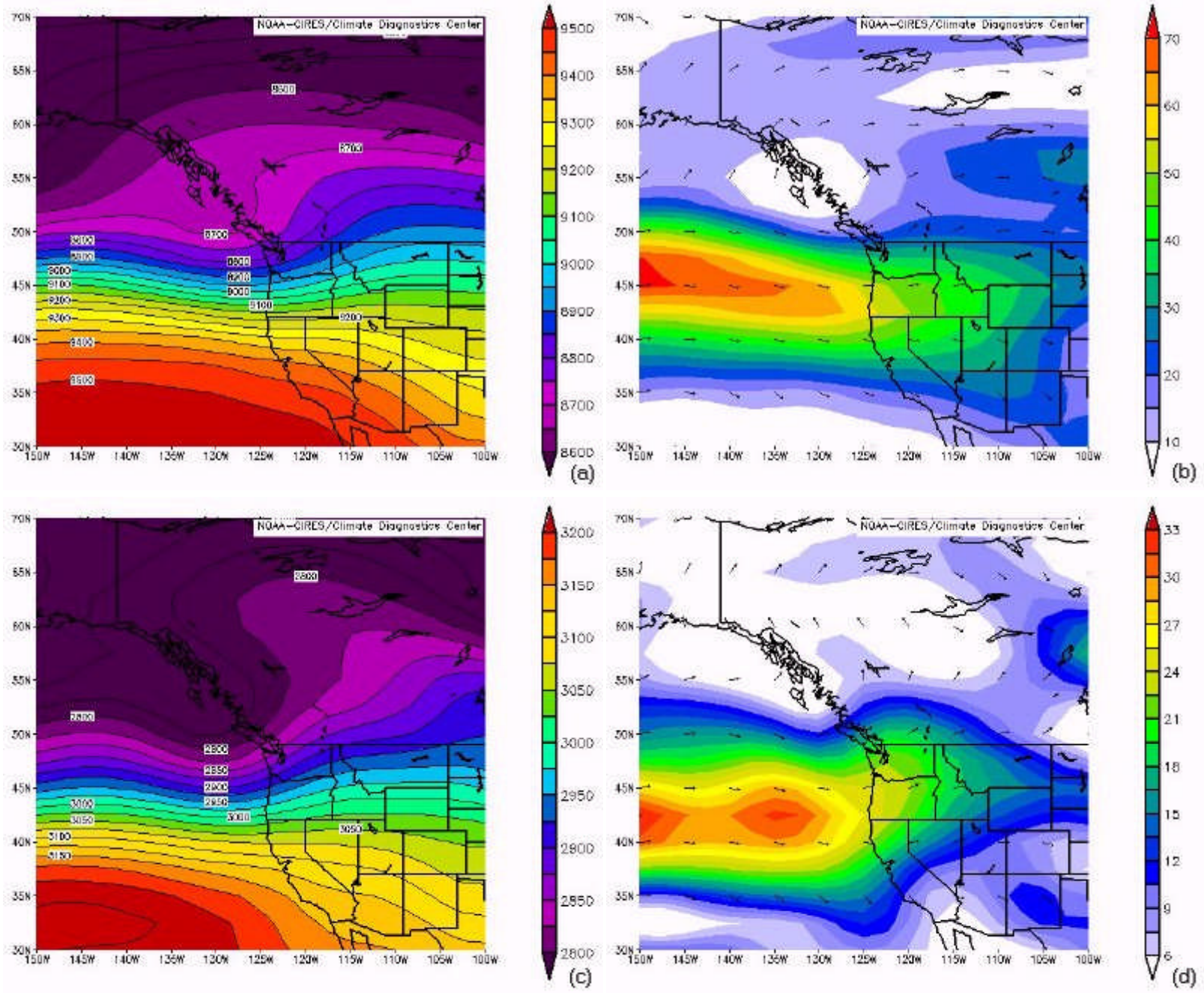

Figure 34: (a) Zonal 300 mb height (m): 1988 March 23
(b) Zonal 300 mb wind speed (m s^{-1}): 1988 March 23
(c) Zonal 700 mb height (m): 1988 March 23
(d) Zonal 700 mb wind speed (m s^{-1}): 1988 March 23